

CERN-EP-2023-046

20 March 2023

Measurement of the angle between jet axes in Pb–Pb collisions at $\sqrt{s_{\text{NN}}} = 5.02 \text{ TeV}$

ALICE Collaboration*

Abstract

This letter presents the first measurement of the angle between different jet axes (denoted as ΔR_{axis}) in Pb–Pb collisions. The measurement is carried out in the 0–10% most-central events at $\sqrt{s_{\text{NN}}} = 5.02 \text{ TeV}$. Jets are assembled by clustering charged particles at midrapidity using the anti- k_T algorithm with resolution parameters $R = 0.2$ and 0.4 and transverse momenta in the intervals $40 < p_T^{\text{ch jet}} < 140 \text{ GeV}/c$ and $80 < p_T^{\text{ch jet}} < 140 \text{ GeV}/c$, respectively. Measurements at these low transverse momenta enhance the sensitivity to quark–gluon plasma (QGP) effects. A comparison to models implementing various mechanisms of jet energy loss in the QGP shows that the observed narrowing of the Pb–Pb distribution relative to pp can be explained if quark-initiated jets are more likely to emerge from the medium than gluon-initiated jets. These new measurements discard intra-jet p_T broadening as described in a model calculation with the BDMPS formalism as the main mechanism of energy loss in the QGP. The data are sensitive to the angular scale at which the QGP can resolve two independent splittings, favoring mechanisms that incorporate incoherent energy loss.

The strongly interacting, deconfined state of matter of our universe a few microseconds after the Big Bang can be recreated in ultrarelativistic heavy-ion collisions at the Large Hadron Collider (LHC) [1, 2]. Studying the microscopic structure of this quark–gluon plasma (QGP) can elucidate the physics of many-body strongly coupled systems [3]. Because droplets of QGP created at colliders are small and short-lived, studying interactions within those droplets requires auto-generated probes. In this study, jets of energetic hadrons, which arise from high-momentum-transfer (hard) collisions between quarks and gluons (partons) in the incoming nuclei, are used. These hard-scattered particles produce showers of secondary partons, which give rise to jets of multiple correlated hadrons (see Fig. 1, left).

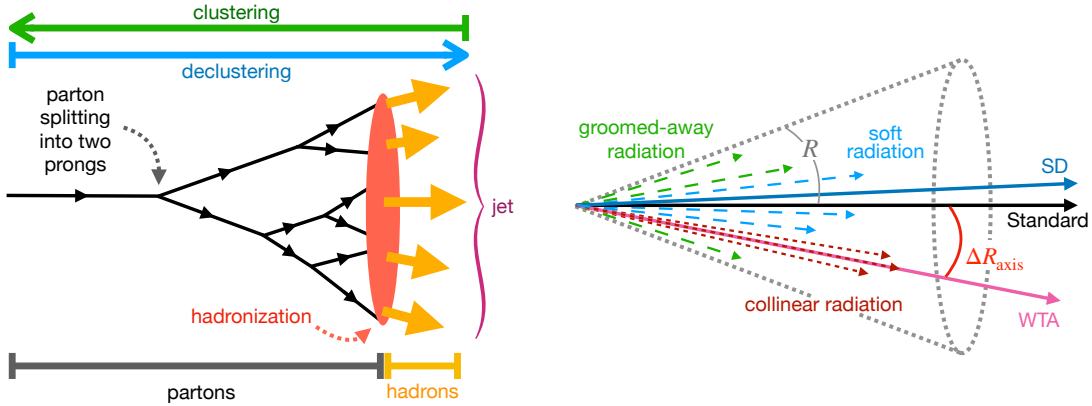


Figure 1: Left: schematic of how energetic partons split or fragment into lower-energy prongs or branches of partons down to a scale in which hadrons emerge. An algorithm can be run over final-state hadrons to cluster them into jets. An inverse declustering algorithm can be used to recursively explore the jet substructure. Right: schematic showing that different jet axes (solid arrows) can be selected from a jet to construct the ΔR_{axis} observable. The Standard axis (represented by a black arrow) is constrained by all the jet constituents (represented by dashed arrows). The SD axis (represented by a dark blue arrow) is determined by the particles left in the jet after grooming (blue and dark red arrows). Finally, the WTA axis (represented by a pink arrow) tends to be aligned with the most energetic constituent.

When traversing the QGP, jets interact with the medium, lose energy, and are modified relative to their structure in elementary (e.g., ee or pp) collisions. Thus, measuring the substructure of jets can provide sensitivity to different scales within the jet modification process. The direction of a jet in rapidity (y) and azimuth (ϕ), referred to as the jet axis, is affected by transverse modification of the partonic shower, with varying sensitivity to soft radiation, depending on how the axis is defined [4].

This letter presents the first measurement in heavy-ion collisions of the angle between pairs of jet axes, ΔR_{axis} (see Fig. 1, right). This observable shows how well the QGP resolves the angular structure of the parton shower [4] and is defined as

$$\Delta R_{\text{axis}} \equiv \sqrt{(y_{\text{axis},1} - y_{\text{axis},2})^2 + (\varphi_{\text{axis},1} - \varphi_{\text{axis},2})^2}, \quad (1)$$

where $y_{\text{axis},i}$ and $\varphi_{\text{axis},i}$ are the rapidity and azimuthal coordinates of the axes, respectively. The axes considered in this analysis are:

- “Standard”: coordinates in $y-\varphi$ of the 4-vector resulting from clustering jets with the anti- k_T algorithm [5] using the E recombination scheme (two branches combined into one by adding their 4-momenta). In this case, all jet constituents including soft (low-transverse-momentum) and hard radiation contribute to the axis.
- “Soft Drop” (SD): coordinates in $y-\varphi$ of jet after soft wide-angle radiation is removed using the Soft Drop grooming procedure [6] with the Cambridge–Aachen (C/A) reclustering algorithm [7,

8]. The procedure stops when a splitting is found that satisfies the condition

$$\frac{\min(p_{T,1}, p_{T,2})}{p_{T,1} + p_{T,2}} > z_{\text{cut}} \left(\frac{\Delta R_{1,2}}{R} \right)^{\beta}, \quad (2)$$

where $p_{T,i}$ are the transverse momenta of each of the two branches in the splitting, $\Delta R_{1,2}$ is the distance between them in the y – φ plane, R is the jet resolution parameter, and z_{cut} and β are user-set parameters.

- “Winner-Takes-All” (WTA): coordinates in y – φ of jet after reclustering its constituents using the C/A algorithm and the WTA p_T recombination scheme [9], which combines two jet branches into one by giving the merged branch the total p_T of the two sub-branches and the direction of the hardest sub-branch. The WTA axis is often consistent with the direction of the hardest constituent of the jet and is insensitive to soft radiation at the leading power of the observable [4].

Measurements of ΔR_{axis} are sensitive to medium-induced effects. For example, an increase in the relative fraction of quark- vs. gluon-initiated jets due to medium-induced radiative energy loss can narrow the angular distribution, while multiple scattering of the hard-scattered parton off medium partons can broaden it [10]. Reference 11 reported a net narrowing of the distribution in Pb–Pb collisions, quantitatively consistent with the former. This can be expected if the broadening was primarily in the wide-angle radiation that grooming removes from the jet. This is tested by looking for broadening effects in an ungroomed angular observable, such as the angle between the Standard and WTA axes.

Measurements of ΔR_{axis} are also sensitive to the wake created by a jet imparting some of its momentum to the QGP. This wake is often referred to as medium response [12] and is expected to dominate at large angles from the Standard axis. Consequently, progressively increasing the grooming intensity, while simultaneously varying the jet resolution parameter R can uncover the medium response effect. Comparing experimental results with different models is expected to disentangle medium response and medium-induced large-angle radiation.

The medium resolution length, L_{res} , is a property of the QGP proportional to the inverse of its local temperature [13]. It characterizes the minimum separation distance at which two color charges within the same jet interact independently with the QGP. Certain groomed substructure observables are sensitive to this scale [14]. In this analysis, the sensitivity of ΔR_{axis} to L_{res} is investigated.

The measured ΔR_{axis} distributions in pp collisions at $\sqrt{s} = 5.02$ TeV reported in Ref. 15 are used as the reference for QGP-induced effects reported here. Perturbative QCD calculations [4] were found to agree with the measurements in pp collisions within the experimental uncertainties, demonstrating good theoretical control of the observables. The data were collected in 2018 from Pb–Pb collisions at a center-of-mass energy per nucleon–nucleon pair of $\sqrt{s_{\text{NN}}} = 5.02$ TeV with the ALICE detector [2]. A detailed description of the detector and its performance can be found in Refs. 16 and 17. A trigger based on the charged-particle multiplicity in the forward region [18] was used to select events in the 0–10% centrality class [19, 20]. The events were required to have a reconstructed primary vertex within ± 10 cm of the nominal interaction point in the longitudinal direction. Beam-induced background events were removed using two Zero Degree Calorimeters and pileup effects were removed by discarding events that contained multiple reconstructed vertices [21]. These selection criteria yield a data sample with 92 million events, corresponding to an integrated luminosity of $\approx 0.12 \text{ nb}^{-1}$.

Charged-particle tracks reconstructed in the Inner Tracking System (ITS) [22] and Time Projection Chamber (TPC) [23] used in the analysis were required to have a transverse momentum $p_T > 0.15 \text{ GeV}/c$ and a pseudorapidity $|\eta| < 0.9$. See the supplemental materials [24] for details. The detector performance was estimated by propagating simulated events through a GEANT 3 [25] model of the ALICE detector. The transverse-momentum resolution $\sigma(p_T)/p_T$ increases linearly from $\approx 1\%$ at $p_T = 1 \text{ GeV}/c$ to $\approx 4\%$

at $p_{\text{T}} = 50$ GeV/ c [17]. The tracking efficiency rapidly increases from $\approx 65\%$ at $p_{\text{T}} = 0.15$ GeV/ c to $\approx 85\%$ at $p_{\text{T}} = 1$ GeV/ c , and remains above $\approx 75\%$ at higher p_{T} . The large uncorrelated background from the underlying event (UE) [26] in high-multiplicity heavy-ion collisions is subtracted before jet finding using the event-wide constituent subtraction procedure from Refs. 27 and 28. The parameters used are $\alpha = 0$, $A_g = 0.01$, and $\Delta R^{\max} = 0.1$ (0.25) when the track sample is used to cluster jets of $R = 0.2$ (0.4).

Tracks included in jet clustering are assigned the charged-pion mass. Charged-particle jets are clustered with the anti- k_{T} algorithm, the E recombination scheme, and resolution parameters $R = 0.2$ and 0.4, using FastJet [29]. Jets containing a track with $p_{\text{T}} > 100$ GeV/ c and jets with their Standard axis not pointing inside the fiducial volume of the TPC ($|\eta_{\text{jet}}| < 0.9 - R$) are discarded.

The measured distributions are unfolded to correct for detector effects as well as residual UE fluctuations using an iterative Bayesian procedure [30, 31]. The procedure uses a 4D response matrix (RM) that captures the correspondence between ΔR_{axis} and jet transverse momentum ($p_{\text{T}}^{\text{ch jet}}$) at the generator and detector levels. The generator-level component of the RM is modeled using generated PYTHIA 8 [32] Monash 2013 [33] events. The detector-level component of the RM is modeled by propagating those events through a GEANT 3 [25] model of the ALICE detector and embedding the smeared events into measured Pb–Pb events.

Systematic uncertainties arise from the tracking inefficiency, unfolding procedure, unfolding model dependence, UE subtraction procedure, and residual effects from combinatorial jets. The tracking-inefficiency uncertainty is determined by repeating the analysis with an RM based on a track sample with 4% of all tracks randomly rejected. This number corresponds to the uncertainty in the tracking efficiency, determined by varying the track selection parameters and ITS–TPC matching criteria.

The unfolding-procedure uncertainty is determined by extending the lower and upper bounds of the $p_{\text{T}}^{\text{ch jet}}$ spectrum by 5 GeV/ c , changing the detector-level ΔR_{axis} binning, changing the number of unfolding iterations, and scaling the prior distribution. The four categories of variations are carried out individually and combined into an unfolding uncertainty using their standard deviation. The uncertainty from the model dependence in the unfolding is determined by repeating the analysis with response matrices based on different event generators including Herwig 7 [34] and JEWEL [35] with and without the inclusion of medium partons recoiling after interactions with the jet.

Potential bias introduced by the event-wide UE subtraction [27, 28] is quantified as the maximum difference between the nominal result and the results obtained by repeating the procedure with parameters $\Delta R^{\max} = 0.05$ (0.1), which lead to an under-subtraction, and $\Delta R^{\max} = 0.5$ (0.7), which lead to an over-subtraction of the background, for jets of $R = 0.2$ (0.4). Deviations between the generator-level and unfolded distributions due to residual combinatorial jets are determined with a closure test. PYTHIA 8 events are embedded into background events with no jets and analyzed identically to the measured data. Deviations between the unfolded and PYTHIA 8 generator-level spectra are assigned as the uncertainty.

The systematic uncertainties are added in quadrature. The total systematic uncertainty is in the range of 2–61% depending on ΔR_{axis} and $p_{\text{T}}^{\text{ch jet}}$. The large variation comes primarily from the background subtraction procedure at low $p_{\text{T}}^{\text{ch jet}}$ (where background effects are largest). It is small at low values of ΔR_{axis} , and smoothly grows in the tails of the distributions. See the supplemental materials [24] for details. The measured distributions are normalized to the total number of jets in a given $p_{\text{T}}^{\text{ch jet}}$ interval, N , which is equivalent to reporting the self-normalized cross section:

$$\frac{1}{N(p_{\text{T}}^{\text{ch jet}})} \frac{dN}{d\Delta R_{\text{axis}}} \left(p_{\text{T}}^{\text{ch jet}} \right) \equiv \frac{1}{\sigma(p_{\text{T}}^{\text{ch jet}})} \frac{d\sigma}{d\Delta R_{\text{axis}}} \left(p_{\text{T}}^{\text{ch jet}} \right). \quad (3)$$

This normalization choice causes the Pb–Pb/pp ratios to go above unity at low ΔR_{axis} . In an absolute cross section measurement, the ratio would be below unity as a result of jet suppression in heavy-ion

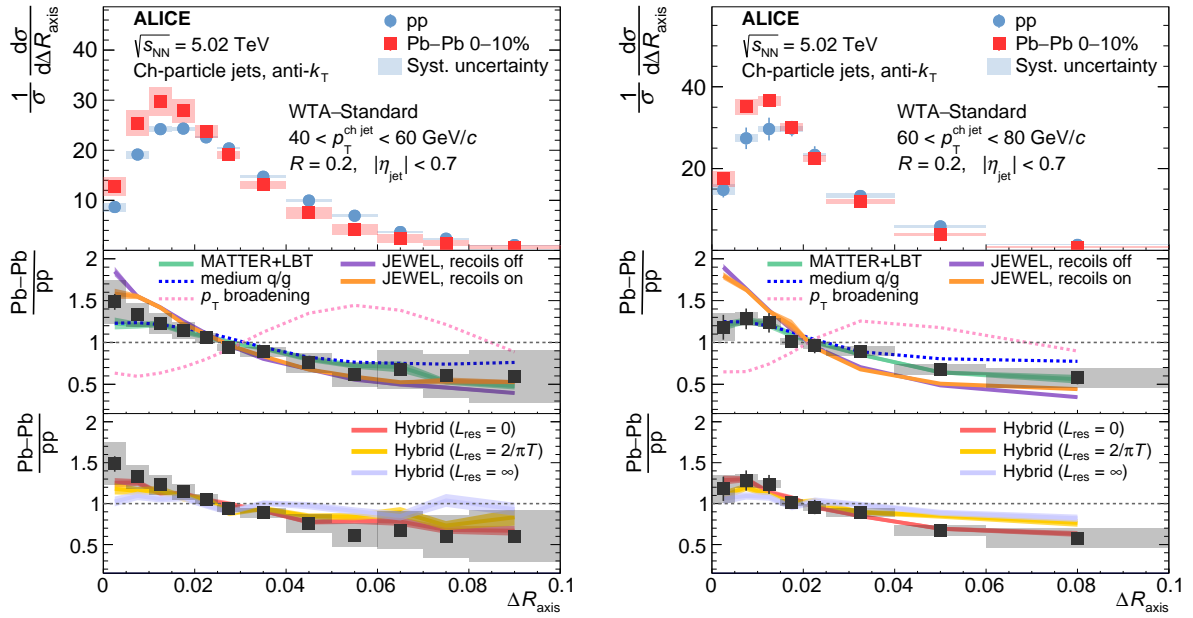


Figure 2: Top panels: fully corrected Pb–Pb and pp ΔR_{axis} distributions in the $p_{\text{T}}^{\text{ch jet}}$ intervals [40, 60] (left), and [60, 80] (right) GeV/c for jets of $R = 0.2$. The pp baseline is taken from Ref. 15. Central and bottom panels: measured Pb–Pb/pp ratio in black, as well as predictions from a selection of jet quenching models.

collisions. The suppression factor was measured in Ref. 36. Thus, only the shape and not the absolute scale of the ΔR_{axis} spectra is reported.

The measured WTA–Standard distributions are shown in Fig. 2 for $R = 0.2$ jets in the $p_{\text{T}}^{\text{ch jet}}$ ranges [40, 60] and [60, 80] GeV/c . The top panels show ΔR_{axis} spectra from Pb–Pb and pp collisions. The vertical error bars represent the statistical uncertainties and the rectangles represent the total systematic uncertainties. The central and bottom panels show the Pb–Pb/pp ratio, with all uncertainties assumed uncorrelated and added in quadrature when calculating the ratio. The equivalent results for other $p_{\text{T}}^{\text{ch jet}}$ ranges, jet resolution parameters, and grooming settings are included in the supplemental materials [24].

The data are compared with several jet quenching models. These models have different implementations of the microscopic properties of the medium, its evolution, and the jet–medium interaction. The **JEWEL** event generator [35] models the medium with a boost-invariant longitudinally expanding ideal quark–gluon gas [37]. Parameters from Ref. 38, which are adequate for the kinematics of this measurement, are used. The medium partons recoiling after interacting with jet constituents can be discarded from the event (recoils off) or allowed to hadronize together with the jet (recoils on). “**MATTER+LBT**” is from the JETSCAPE event generator [39, 40], implementing an in-medium parton shower with interactions of high- (low-) virtuality partons with the medium described by the MATTER [41] (Linear Boltzmann Transport [42]) model. The curve labeled “**medium q/g**” corresponds to a phenomenological model in which the only difference between the Pb–Pb and pp results comes from a modification of the fraction of quarks and gluons that initiate the jets [43, 44], highlighting that these two jet populations lose energy differently in the medium. The “**p_T broadening**” calculation adds to the previous model a p_{T} broadening caused by incoherent multiple scatterings with the medium partons [10] following the BDMPS approach [45–47]. This calculation uses a mean square momentum transfer coefficient between the jet and medium constituents $\langle \hat{q}L \rangle = 5 \text{ GeV}^2$. “**Hybrid**” is from the hybrid model [48], which describes the weakly coupled jet showering process using the DGLAP formalism and the strongly coupled interaction between the jet constituents and medium partons via holographic calculations of energy loss based on AdS/CFT. The case $L_{\text{res}} = 0$ corresponds to fully incoherent energy loss, where the medium is able to resolve the splitting immediately after the parton fragments, resulting in higher energy loss [13].

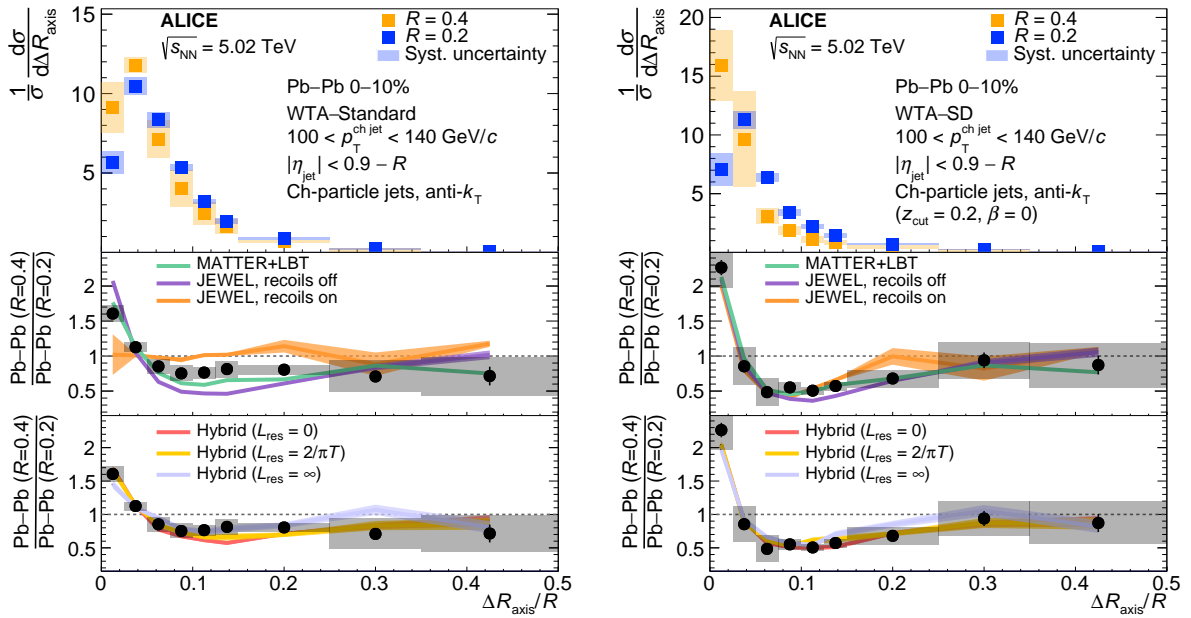


Figure 3: Top panels: fully corrected Pb–Pb $\Delta R_{\text{axis}}^{\text{WTA-Standard}}/R$ (left), and $\Delta R_{\text{axis}}^{\text{WTA-SD}}/R$ with ($z_{\text{cut}} = 0.2, \beta = 0$) (right) distributions in the $p_{\text{T}}^{\text{ch jet}}$ interval [100, 140] GeV/c. Central and bottom panels: measured Pb–Pb($R = 0.4$)/Pb–Pb($R = 0.2$) ratio in black, as well as predictions from a selection of jet quenching models.

The case $L_{\text{res}} = \infty$ corresponds to fully coherent energy loss, where the medium is not able to resolve splittings, and the energy loss is lower. The intermediate case $L_{\text{res}} = 2/\pi T$, where T is the medium local temperature, is also included. All “Hybrid” curves include medium-response effects from Ref. 49.

The measured $R = 0.2$ distributions are narrower than those measured in pp collisions. Results with $R = 0.4$, presented in the supplemental materials [24], are consistent with this narrowing, but also with no modification within statistical and systematic uncertainties. The narrowing may be due to a selection bias, as jets selected using $p_{\text{T}}^{\text{ch jet}}$ (rather than the initial momentum before the jet-medium interactions, which is not accessible experimentally) tend to lose little energy in the QGP [50]. Similarly, the experimental result is also consistent with a quark-enhanced mixture of jets surviving the interaction with the medium relative to the vacuum case, as expected since gluon-initiated jets couple more strongly to partons of the QGP and thus lose more energy [11, 43, 51]. The MATTER+LBT model overall describes the data for all considered kinematical regions.

In contrast with $R = 0.2$, for larger R there are significant differences in JEWEL predictions with and without recoils. This is expected, as the medium response populates larger angles away from the Standard jet axis. However, grooming reduces the sensitivity to the medium response. The Hybrid model does not predict a significant effect from the medium response. See the supplemental materials [24] for details. The inclusion of other models in which the medium response can be turned on and off (e.g. Co-LBT [52, 53]) could help clarify the sensitivity of ΔR_{axis} to the properties and magnitude of this effect. Narrowing of the distributions relative to those measured in pp collisions for jets of $R = 0.2$ is qualitatively predicted by all models except for “ p_{T} broadening”. This excludes the hypothesis that intra-jet p_{T} broadening manifests in the groomed radiation in previous measurements [11].

The data are closest to incoherent energy loss of jets in the Hybrid model ($L_{\text{res}} = 0$). The fully coherent case ($L_{\text{res}} = \infty$) predicts significantly less narrowing. Fully incoherent energy loss better reproduces the data than the intermediate case of $L_{\text{res}} = 2/\pi T$. In holographic calculations of the Debye screening length, the intermediate case is expected to be closer to the true medium resolution scale [13].

The precision of the data at higher $p_{\text{T}}^{\text{ch jet}}$ is limited by the integrated luminosity of the pp dataset, which

only allows for an extraction of the Pb–Pb/pp results up to 100 GeV/ c . However, in heavy-ion collisions, larger $p_T^{\text{ch,jet}}$ can be studied through the ratio of $(R = 0.4)/(R = 0.2)$ spectra, where the systematic uncertainties partially cancel. This kinematic range is also important for future comparisons with results from other experiments which cannot access the low- p_T regime of this measurement. The ratio is reported as a function of the jet angular scale $\Delta R_{\text{axis}}/R$ that, by construction, is independent of R . Figure 3 shows the ratio for $p_T^{\text{ch,jet}} \in [100, 140]$ GeV/ c together with theoretical predictions. The ungroomed WTA–Standard result is challenging to models, as can be seen in Fig. 3 (left). Grooming improves the agreement between the models and the data (see Fig. 3 (right)), suggesting that the ungroomed result captures significantly more of the non-perturbative aspects of jet quenching.

Comparing $\Delta R_{\text{axis}}^{\text{WTA-Standard}}$ to $\Delta R_{\text{axis}}^{\text{WTA-SD}}$ with different grooming settings shows that grooming does not significantly impact the experimental results. This is similar to pp collisions, where the Standard and SD axes were found more aligned with each other than either of them with the WTA axis. While the Standard axis is influenced by the soft wide-angle radiation groomed away in the SD-axis case, it is dominated by the hard radiation that remains in the SD case.

In summary, the first measurement of the angle between the WTA and Standard or Soft Drop groomed charged-particle jet axes in Pb–Pb collisions is reported. The measurement was carried out using 0–10% most-central collisions at $\sqrt{s_{\text{NN}}} = 5.02$ TeV with the ALICE detector and for $p_T^{\text{ch,jet}} \in [40, 140]$ ([80, 140]) GeV/ c for jets of $R = 0.2$ (0.4).

Narrowing of the ΔR_{axis} distribution relative to the vacuum case is found. The narrowing may be explained if the Pb–Pb distribution is dominated by quark-initiated jets, since gluon-initiated jets are expected to interact more with the medium. This is consistent with the prediction from the “medium q/g” model. The measurement disfavors intra-jet p_T broadening, as implemented in Ref. 10.

The ΔR_{axis} observables exhibit sensitivity to the medium resolution length. The measurement favors incoherent energy loss of jets, where the medium resolves a splitting immediately after it happens, regardless of the angular separation between the prongs. Future measurements of ΔR_{axis} in photon- or Z-boson-tagged jets could provide a way to experimentally vary the fraction of quark- vs. gluon-initiated jets.

Acknowledgements

We gratefully acknowledge Felix Ringer, Daniel Pablos, and the JETSCAPE collaboration for providing theoretical predictions. We also acknowledge Xin-Nian Wang and Feng Yuan for fruitful discussions.

The ALICE Collaboration would like to thank all its engineers and technicians for their invaluable contributions to the construction of the experiment and the CERN accelerator teams for the outstanding performance of the LHC complex. The ALICE Collaboration gratefully acknowledges the resources and support provided by all Grid centres and the Worldwide LHC Computing Grid (WLCG) collaboration. The ALICE Collaboration acknowledges the following funding agencies for their support in building and running the ALICE detector: A. I. Alikhanyan National Science Laboratory (Yerevan Physics Institute) Foundation (ANSL), State Committee of Science and World Federation of Scientists (WFS), Armenia; Austrian Academy of Sciences, Austrian Science Fund (FWF): [M 2467-N36] and Nationalstiftung für Forschung, Technologie und Entwicklung, Austria; Ministry of Communications and High Technologies, National Nuclear Research Center, Azerbaijan; Conselho Nacional de Desenvolvimento Científico e Tecnológico (CNPq), Financiadora de Estudos e Projetos (Finep), Fundação de Amparo à Pesquisa do Estado de São Paulo (FAPESP) and Universidade Federal do Rio Grande do Sul (UFRGS), Brazil; Bulgarian Ministry of Education and Science, within the National Roadmap for Research Infrastructures 2020;2027 (object CERN), Bulgaria; Ministry of Education of China (MOEC) , Ministry of Science & Technology of China (MSTC) and National Natural Science Foundation of China (NSFC),

China; Ministry of Science and Education and Croatian Science Foundation, Croatia; Centro de Aplicaciones Tecnológicas y Desarrollo Nuclear (CEADEN), Cubaenergía, Cuba; Ministry of Education, Youth and Sports of the Czech Republic, Czech Republic; The Danish Council for Independent Research — Natural Sciences, the VILLUM FONDEN and Danish National Research Foundation (DNRF), Denmark; Helsinki Institute of Physics (HIP), Finland; Commissariat à l’Energie Atomique (CEA) and Institut National de Physique Nucléaire et de Physique des Particules (IN2P3) and Centre National de la Recherche Scientifique (CNRS), France; Bundesministerium für Bildung und Forschung (BMBF) and GSI Helmholtzzentrum für Schwerionenforschung GmbH, Germany; General Secretariat for Research and Technology, Ministry of Education, Research and Religions, Greece; National Research, Development and Innovation Office, Hungary; Department of Atomic Energy Government of India (DAE), Department of Science and Technology, Government of India (DST), University Grants Commission, Government of India (UGC) and Council of Scientific and Industrial Research (CSIR), India; National Research and Innovation Agency - BRIN, Indonesia; Istituto Nazionale di Fisica Nucleare (INFN), Italy; Japanese Ministry of Education, Culture, Sports, Science and Technology (MEXT) and Japan Society for the Promotion of Science (JSPS) KAKENHI, Japan; Consejo Nacional de Ciencia (CONACYT) y Tecnología, through Fondo de Cooperación Internacional en Ciencia y Tecnología (FONCICYT) and Dirección General de Asuntos del Personal Académico (DGAPA), Mexico; Nederlandse Organisatie voor Wetenschappelijk Onderzoek (NWO), Netherlands; The Research Council of Norway, Norway; Commission on Science and Technology for Sustainable Development in the South (COMSATS), Pakistan; Pontificia Universidad Católica del Perú, Peru; Ministry of Education and Science, National Science Centre and WUT ID-UB, Poland; Korea Institute of Science and Technology Information and National Research Foundation of Korea (NRF), Republic of Korea; Ministry of Education and Scientific Research, Institute of Atomic Physics, Ministry of Research and Innovation and Institute of Atomic Physics and University Politehnica of Bucharest, Romania; Ministry of Education, Science, Research and Sport of the Slovak Republic, Slovakia; National Research Foundation of South Africa, South Africa; Swedish Research Council (VR) and Knut & Alice Wallenberg Foundation (KAW), Sweden; European Organization for Nuclear Research, Switzerland; Suranaree University of Technology (SUT), National Science and Technology Development Agency (NSTDA), Thailand Science Research and Innovation (TSRI) and National Science, Research and Innovation Fund (NSRF), Thailand; Turkish Energy, Nuclear and Mineral Research Agency (TENMAK), Turkey; National Academy of Sciences of Ukraine, Ukraine; Science and Technology Facilities Council (STFC), United Kingdom; National Science Foundation of the United States of America (NSF) and United States Department of Energy, Office of Nuclear Physics (DOE NP), United States of America. In addition, individual groups or members have received support from: European Research Council, Strong 2020 - Horizon 2020 (grant nos. 950692, 824093), European Union; Academy of Finland (Center of Excellence in Quark Matter) (grant nos. 346327, 346328), Finland; Programa de Apoyos para la Superación del Personal Académico, UNAM, Mexico.

References

- [1] W. Busza, K. Rajagopal, and W. van der Schee, “Heavy Ion Collisions: The Big Picture, and the Big Questions”, *Ann. Rev. Nucl. Part. Sci.* **68** (2018) 339–376, arXiv:1802.04801 [hep-ph].
- [2] ALICE Collaboration, “The ALICE experiment – A journey through QCD”, arXiv:2211.04384 [nucl-ex].
- [3] B. V. Jacak and B. Müller, “The exploration of hot nuclear matter”, *Science* **337** (2012) 310–314.
- [4] P. Cal, D. Neill, F. Ringer, and W. J. Waalewijn, “Calculating the angle between jet axes”, *JHEP* **04** (2020) 211, arXiv:1911.06840 [hep-ph].
- [5] M. Cacciari, G. P. Salam, and G. Soyez, “The anti- k_t jet clustering algorithm”, *JHEP* **04** (2008) 063, arXiv:0802.1189 [hep-ph].

- [6] A. J. Larkoski, S. Marzani, G. Soyez, and J. Thaler, “Soft Drop”, *JHEP* **05** (2014) 146, arXiv:1402.2657 [hep-ph].
- [7] Y. L. Dokshitzer, G. D. Leder, S. Moretti, and B. R. Webber, “Better jet clustering algorithms”, *JHEP* **08** (1997) 001, arXiv:hep-ph/9707323.
- [8] M. Wobisch and T. Wengler, “Hadronization corrections to jet cross-sections in deep inelastic scattering”, in *Workshop on Monte Carlo Generators for HERA Physics (Plenary Starting Meeting)*, pp. 270–279. 4, 1998. arXiv:hep-ph/9907280.
- [9] D. Bertolini, T. Chan, and J. Thaler, “Jet Observables Without Jet Algorithms”, *JHEP* **04** (2014) 013, arXiv:1310.7584 [hep-ph].
- [10] F. Ringer, B.-W. Xiao, and F. Yuan, “Can we observe jet P_T -broadening in heavy-ion collisions at the LHC?”, *Phys. Lett. B* **808** (2020) 135634, arXiv:1907.12541 [hep-ph].
- [11] ALICE Collaboration, S. Acharya *et al.*, “Measurement of the groomed jet radius and momentum splitting fraction in pp and Pb–Pb collisions at $\sqrt{s_{\text{NN}}} = 5.02$ TeV”, *Phys. Rev. Lett.* **128** (2022) 102001, arXiv:2107.12984 [nucl-ex].
- [12] G. Milhano, U. A. Wiedemann, and K. C. Zapp, “Sensitivity of jet substructure to jet-induced medium response”, *Phys. Lett. B* **779** (2018) 409–413, arXiv:1707.04142 [hep-ph].
- [13] Z. Hulcher, D. Pablos, and K. Rajagopal, “Resolution Effects in the Hybrid Strong/Weak Coupling Model”, *JHEP* **03** (2018) 010, arXiv:1707.05245 [hep-ph].
- [14] J. Casalderrey-Solana, J. G. Milhano, D. Pablos, and K. Rajagopal, “Modification of Jet Substructure in Heavy Ion Collisions as a Probe of the Resolution Length of Quark-Gluon Plasma”, *JHEP* **2020** (2020) 044, arXiv:1907.11248 [hep-ph].
- [15] ALICE Collaboration, “Measurement of the angle between jet axes in pp collisions at $\sqrt{s} = 5.02$ TeV”, arXiv:2211.08928 [nucl-ex].
- [16] ALICE Collaboration, K. Aamodt *et al.*, “The ALICE experiment at the CERN LHC”, *JINST* **3** (2008) S08002.
- [17] ALICE Collaboration, B. Abelev *et al.*, “Performance of the ALICE Experiment at the CERN LHC”, *Int. J. Mod. Phys. A* **29** (2014) 1430044, arXiv:1402.4476 [nucl-ex].
- [18] ALICE Collaboration, E. Abbas *et al.*, “Performance of the ALICE VZERO system”, *JINST* **8** (2013) P10016, arXiv:1306.3130 [nucl-ex].
- [19] ALICE Collaboration, B. Abelev *et al.*, “Centrality determination of Pb–Pb collisions at $\sqrt{s_{\text{NN}}} = 2.76$ TeV with ALICE”, *Phys. Rev. C* **88** (2013) 044909, arXiv:1301.4361 [nucl-ex].
- [20] ALICE Collaboration, “Centrality determination in heavy ion collisions”, *ALICE-PUBLIC-2018-011* (2018) . <https://cds.cern.ch/record/2636623>.
- [21] ALICE Collaboration, S. Acharya *et al.*, “Measurements of inclusive jet spectra in pp and central Pb–Pb collisions at $\sqrt{s_{\text{NN}}} = 5.02$ TeV”, *Phys. Rev. C* **101** (2020) 034911, arXiv:1909.09718 [nucl-ex].
- [22] ALICE Collaboration, K. Aamodt *et al.*, “Alignment of the ALICE Inner Tracking System with cosmic-ray tracks”, *JINST* **5** (2010) P03003, arXiv:1001.0502 [physics.ins-det].

- [23] J. Alme *et al.*, “The ALICE TPC, a large 3-dimensional tracking device with fast readout for ultra-high multiplicity events”, *Nucl. Instrum. Meth. A* **622** (2010) 316–367, arXiv:1001.1950 [physics.ins-det].
- [24] ALICE Collaboration, “Supplemental materials: Measurement of the angle between jet axes in Pb–Pb collisions at $\sqrt{s_{\text{NN}}} = 5.02$ TeV”, <https://cds.cern.ch/record/2852587/files.CERN-EP-2023-046>.
- [25] R. Brun, F. Bruyant, M. Maire, A. C. McPherson, and P. Zanarini, *GEANT 3: user’s guide Geant 3.10, Geant 3.11; rev. version*. CERN, Geneva, Sep, 1987. <https://cds.cern.ch/record/1119728>.
- [26] ALICE Collaboration, B. Abelev *et al.*, “Measurement of Event Background Fluctuations for Charged Particle Jet Reconstruction in Pb–Pb collisions at $\sqrt{s_{\text{NN}}} = 2.76$ TeV”, *JHEP* **03** (2012) 053, arXiv:1201.2423 [hep-ex].
- [27] P. Berta, M. Spousta, D. W. Miller, and R. Leitner, “Particle-level pileup subtraction for jets and jet shapes”, *JHEP* **06** (2014) 092, arXiv:1403.3108 [hep-ex].
- [28] P. Berta, L. Masetti, D. W. Miller, and M. Spousta, “Pileup and Underlying Event Mitigation with Iterative Constituent Subtraction”, *JHEP* **08** (2019) 175, arXiv:1905.03470 [hep-ph].
- [29] M. Cacciari, G. P. Salam, and G. Soyez, “FastJet User Manual”, *Eur. Phys. J. C* **72** (2012) 1896, arXiv:1111.6097 [hep-ph].
- [30] G. D’Agostini, “A multidimensional unfolding method based on Bayes’ theorem”, *Nucl. Instrum. Meth. A* **362** (1994) 487 – 498.
- [31] G. D’Agostini, “Improved iterative Bayesian unfolding”, in *Alliance Workshop on Unfolding and Data Correction*. 10, 2010. arXiv:1010.0632 [physics.data-an].
- [32] T. Sjöstrand, S. Ask, J. R. Christiansen, R. Corke, N. Desai, P. Ilten, S. Mrenna, S. Prestel, C. O. Rasmussen, and P. Z. Skands, “An introduction to PYTHIA 8.2”, *Comput. Phys. Commun.* **191** (2015) 159–177, arXiv:1410.3012 [hep-ph].
- [33] P. Skands, S. Carrazza, and J. Rojo, “Tuning PYTHIA 8.1: the Monash 2013 Tune”, *Eur. Phys. J. C* **74** (2014) 3024, arXiv:1404.5630 [hep-ph].
- [34] S. Gieseke, C. Rohr, and A. Siodmok, “Colour reconnections in Herwig++”, *Eur. Phys. J. C* **72** (2012) 2225, arXiv:1206.0041 [hep-ph].
- [35] K. C. Zapp, “JEWEL 2.0.0: directions for use”, *Eur. Phys. J. C* **74** (2014) 2762, arXiv:1311.0048 [hep-ph].
- [36] ALICE Collaboration, “Measurement of the radius dependence of charged-particle jet suppression in Pb-Pb collisions at $\sqrt{s_{\text{NN}}} = 5.02$ TeV”, arXiv:2303.00592 [nucl-ex].
- [37] K. C. Zapp, F. Krauss, and U. A. Wiedemann, “A perturbative framework for jet quenching”, *JHEP* **03** (2013) 080, arXiv:1212.1599 [hep-ph].
- [38] R. Kunawalkam Elayavalli and K. C. Zapp, “Medium response in JEWEL and its impact on jet shape observables in heavy ion collisions”, *JHEP* **07** (2017) 141, arXiv:1707.01539 [hep-ph].
- [39] J. H. Putschke *et al.*, “The JETSCAPE framework”, arXiv:1903.07706 [nucl-th].
- [40] JETSCAPE Collaboration, A. Kumar *et al.*, “Inclusive Jet and Hadron Suppression in a Multi-Stage Approach”, arXiv:2204.01163 [hep-ph].

- [41] A. Majumder, “Incorporating Space-Time Within Medium-Modified Jet Event Generators”, *Phys. Rev. C* **88** (2013) 014909, arXiv:1301.5323 [nucl-th].
- [42] Y. He, T. Luo, X.-N. Wang, and Y. Zhu, “Linear Boltzmann Transport for Jet Propagation in the Quark-Gluon Plasma: Elastic Processes and Medium Recoil”, *Phys. Rev. C* **91** (2015) 054908, arXiv:1503.03313 [nucl-th]. [Erratum: *Phys. Rev. C* **97** (2018), 019902].
- [43] J.-W. Qiu, F. Ringer, N. Sato, and P. Zurita, “Factorization of jet cross sections in heavy-ion collisions”, *Phys. Rev. Lett.* **122** (2019) 252301, arXiv:1903.01993 [hep-ph].
- [44] J.-W. Qiu, F. Ringer, N. Sato, and P. Zurita, “QCD factorization and universality of jet cross sections in heavy-ion collisions”, *Nucl. Phys. A* **1005** (2021) 121853, arXiv:2002.01652 [hep-ph].
- [45] R. Baier, Y. L. Dokshitzer, A. H. Mueller, S. Peigne, and D. Schiff, “Radiative energy loss of high-energy quarks and gluons in a finite volume quark–gluon plasma”, *Nucl. Phys. B* **483** (1997) 291–320, arXiv:hep-ph/9607355.
- [46] R. Baier, Y. L. Dokshitzer, A. H. Mueller, S. Peigne, and D. Schiff, “Radiative energy loss and p(T) broadening of high-energy partons in nuclei”, *Nucl. Phys. B* **484** (1997) 265–282, arXiv:hep-ph/9608322.
- [47] R. Baier, Y. L. Dokshitzer, A. H. Mueller, and D. Schiff, “Medium induced radiative energy loss: Equivalence between the BDMPS and Zakharov formalisms”, *Nucl. Phys. B* **531** (1998) 403–425, arXiv:hep-ph/9804212.
- [48] J. Casalderrey-Solana, D. C. Gulhan, J. G. Milhano, D. Pablos, and K. Rajagopal, “A Hybrid Strong/Weak Coupling Approach to Jet Quenching”, *JHEP* **10** (2014) 019, arXiv:1405.3864 [hep-ph]. [Erratum: JHEP 09, 175 (2015)].
- [49] J. Casalderrey-Solana, D. C. Gulhan, J. G. Milhano, D. Pablos, and K. Rajagopal, “Angular Structure of Jet Quenching Within a Hybrid Strong/Weak Coupling Model”, *JHEP* **03** (2017) 135, arXiv:1609.05842 [hep-ph].
- [50] J. Brewer, Q. Brodsky, and K. Rajagopal, “Disentangling jet modification in jet simulations and in Z+jet data”, *JHEP* **02** (2022) 175, arXiv:2110.13159 [hep-ph].
- [51] M. Spousta and B. Cole, “Interpreting single jet measurements in Pb + Pb collisions at the LHC”, *Eur. Phys. J. C* **76** (2016) 50, arXiv:1504.05169 [hep-ph].
- [52] W. Chen, S. Cao, T. Luo, L.-G. Pang, and X.-N. Wang, “Effects of jet-induced medium excitation in γ -hadron correlation in A+A collisions”, *Phys. Lett. B* **777** (2018) 86–90, arXiv:1704.03648 [nucl-th].
- [53] W. Zhao, W. Ke, W. Chen, T. Luo, and X.-N. Wang, “From Hydrodynamics to Jet Quenching, Coalescence, and Hadron Cascade: A Coupled Approach to Solving the RAA \otimes v2 Puzzle”, *Phys. Rev. Lett.* **128** (2022) 022302, arXiv:2103.14657 [hep-ph].

A The ALICE Collaboration

S. Acharya ¹²⁵, D. Adamová ⁸⁶, A. Adler⁶⁹, G. Aglieri Rinella ³², M. Agnello ²⁹, N. Agrawal ⁵⁰, Z. Ahammed ¹³², S. Ahmad ¹⁵, S.U. Ahn ⁷⁰, I. Ahuja ³⁷, A. Akindinov ¹⁴⁰, M. Al-Turany ⁹⁷, D. Aleksandrov ¹⁴⁰, B. Alessandro ⁵⁵, H.M. Alfanda ⁶, R. Alfaro Molina ⁶⁶, B. Ali ¹⁵, A. Alici ²⁵, N. Alizadehvandchali ¹¹⁴, A. Alkin ³², J. Alme ²⁰, G. Alocco ⁵¹, T. Alt ⁶³, I. Altsybeev ¹⁴⁰, M.N. Anaam ⁶, C. Andrei ⁴⁵, A. Andronic ¹³⁵, V. Anguelov ⁹⁴, F. Antinori ⁵³, P. Antonioli ⁵⁰, N. Apadula ⁷⁴, L. Aphecetche ¹⁰³, H. Appelshäuser ⁶³, C. Arata ⁷³, S. Arcelli ²⁵, M. Aresti ⁵¹, R. Arnaldi ⁵⁵, J.G.M.C.A. Arneiro ¹¹⁰, I.C. Arsene ¹⁹, M. Arslanbekov ¹³⁷, A. Augustinus ³², R. Averbeck ⁹⁷, M.D. Azmi ¹⁵, A. Badalà ⁵², J. Bae ¹⁰⁴, Y.W. Baek ⁴⁰, X. Bai ¹¹⁸, R. Bailhache ⁶³, Y. Bailung ⁴⁷, A. Balbino ²⁹, A. Baldissari ¹²⁸, B. Balis ², D. Banerjee ⁴, Z. Banoo ⁹¹, R. Barbera ²⁶, F. Barile ³¹, L. Barioglio ⁹⁵, M. Barlou ⁷⁸, G.G. Barnaföldi ¹³⁶, L.S. Barnby ⁸⁵, V. Barret ¹²⁵, L. Barreto ¹¹⁰, C. Bartels ¹¹⁷, K. Barth ³², E. Bartsch ⁶³, N. Bastid ¹²⁵, S. Basu ⁷⁵, G. Batigne ¹⁰³, D. Battistini ⁹⁵, B. Batyunya ¹⁴¹, D. Bauri ⁴⁶, J.L. Bazo Alba ¹⁰¹, I.G. Bearden ⁸³, C. Beattie ¹³⁷, P. Becht ⁹⁷, D. Behera ⁴⁷, I. Belikov ¹²⁷, A.D.C. Bell Hechavarria ¹³⁵, F. Bellini ²⁵, R. Bellwied ¹¹⁴, S. Belokurova ¹⁴⁰, G. Bencedi ¹³⁶, S. Beole ²⁴, A. Bercuci ⁴⁵, Y. Berdnikov ¹⁴⁰, A. Berdnikova ⁹⁴, L. Bergmann ⁹⁴, M.G. Besiou ⁶², L. Betev ³², P.P. Bhaduri ¹³², A. Bhasin ⁹¹, M.A. Bhat ⁴, B. Bhattacharjee ⁴¹, L. Bianchi ²⁴, N. Bianchi ⁴⁸, J. Bielčík ³⁵, J. Bielčíková ⁸⁶, J. Biernat ¹⁰⁷, A.P. Bigot ¹²⁷, A. Bilandzic ⁹⁵, G. Biro ¹³⁶, S. Biswas ⁴, N. Bize ¹⁰³, J.T. Blair ¹⁰⁸, D. Blau ¹⁴⁰, M.B. Blidaru ⁹⁷, N. Bluhme ³⁸, C. Blume ⁶³, G. Boca ^{21,54}, F. Bock ⁸⁷, T. Bodova ²⁰, A. Bogdanov ¹⁴⁰, S. Boi ²², J. Bok ⁵⁷, L. Boldizsár ¹³⁶, M. Bombara ³⁷, P.M. Bond ³², G. Bonomi ^{131,54}, H. Borel ¹²⁸, A. Borissov ¹⁴⁰, H. Bossi ¹³⁷, E. Botta ²⁴, Y.E.M. Bouziani ⁶³, L. Bratrud ⁶³, P. Braun-Munzinger ⁹⁷, M. Bregant ¹¹⁰, M. Broz ³⁵, G.E. Bruno ^{96,31}, M.D. Buckland ²³, D. Budnikov ¹⁴⁰, H. Buesching ⁶³, S. Bufalino ²⁹, P. Buhler ¹⁰², Z. Buthelezi ^{67,121}, A. Bylinkin ²⁰, S.A. Bysiak ¹⁰⁷, M. Cai ⁶, H. Caines ¹³⁷, A. Caliva ²⁸, E. Calvo Villar ¹⁰¹, J.M.M. Camacho ¹⁰⁹, P. Camerini ²³, F.D.M. Canedo ¹¹⁰, M. Carabas ¹²⁴, A.A. Carballo ³², A.G.B. Carcamo ⁹⁴, F. Carnesecchi ³², R. Caron ¹²⁶, L.A.D. Carvalho ¹¹⁰, J. Castillo Castellanos ¹²⁸, F. Catalano ^{32,24}, C. Ceballos Sanchez ¹⁴¹, I. Chakaberia ⁷⁴, P. Chakraborty ⁴⁶, S. Chandra ¹³², S. Chapelain ³², M. Chartier ¹¹⁷, S. Chattopadhyay ¹³², S. Chattopadhyay ⁹⁹, T.G. Chavez ⁴⁴, T. Cheng ^{97,6}, C. Cheshkov ¹²⁶, B. Cheynis ¹²⁶, V. Chibante Barroso ³², D.D. Chinellato ¹¹¹, E.S. Chizzali ⁹⁵, J. Cho ⁵⁷, S. Cho ⁵⁷, P. Chochula ³², P. Christakoglou ⁸⁴, C.H. Christensen ⁸³, P. Christiansen ⁷⁵, T. Chujo ¹²³, M. Ciacco ²⁹, C. Ciccalo ⁵¹, F. Cindolo ⁵⁰, M.R. Ciupek ⁹⁷, G. Clai^{II,50}, F. Colamaria ⁴⁹, J.S. Colburn ¹⁰⁰, D. Colella ^{96,31}, M. Colocci ²⁵, G. Conesa Balbastre ⁷³, Z. Conesa del Valle ⁷², G. Contin ²³, J.G. Contreras ³⁵, M.L. Coquet ¹²⁸, T.M. Cormier ^{1,87}, P. Cortese ^{130,55}, M.R. Cosentino ¹¹², F. Costa ³², S. Costanza ^{21,54}, C. Cot ⁷², J. Crkovská ⁹⁴, P. Crochet ¹²⁵, R. Cruz-Torres ⁷⁴, P. Cui ⁶, A. Dainese ⁵³, M.C. Danisch ⁹⁴, A. Danu ⁶², P. Das ⁸⁰, P. Das ⁴, S. Das ⁴, A.R. Dash ¹³⁵, S. Dash ⁴⁶, A. De Caro ²⁸, G. de Cataldo ⁴⁹, J. de Cuveland ³⁸, A. De Falco ²², D. De Gruttola ²⁸, N. De Marco ⁵⁵, C. De Martin ²³, S. De Pasquale ²⁸, R. Deb ¹³¹, S. Deb ⁴⁷, K.R. Deja ¹³³, R. Del Grande ⁹⁵, L. Dello Stritto ²⁸, W. Deng ⁶, P. Dhankher ¹⁸, D. Di Bari ³¹, A. Di Mauro ³², B. Diab ¹²⁸, R.A. Diaz ^{141,7}, T. Dietel ¹¹³, Y. Ding ⁶, R. Divià ³², D.U. Dixit ¹⁸, Ø. Djupsland ²⁰, U. Dmitrieva ¹⁴⁰, A. Dobrin ⁶², B. Dönigus ⁶³, J.M. Dubinski ¹³³, A. Dubla ⁹⁷, S. Dudi ⁹⁰, P. Dupieux ¹²⁵, M. Durkac ¹⁰⁶, N. Dzalaiova ¹², T.M. Eder ¹³⁵, R.J. Ehlers ⁷⁴, F. Eisenhut ⁶³, D. Elia ⁴⁹, B. Erazmus ¹⁰³, F. Ercolelli ²⁵, F. Erhardt ⁸⁹, M.R. Ersdal ²⁰, B. Espagnon ⁷², G. Eulisse ³², D. Evans ¹⁰⁰, S. Evdokimov ¹⁴⁰, L. Fabbietti ⁹⁵, M. Faggin ²⁷, J. Faivre ⁷³, F. Fan ⁶, W. Fan ⁷⁴, A. Fantoni ⁴⁸, M. Fasel ⁸⁷, P. Fecchio ²⁹, A. Feliciello ⁵⁵, G. Feofilov ¹⁴⁰, A. Fernández Téllez ⁴⁴, L. Ferrandi ¹¹⁰, M.B. Ferrer ³², A. Ferrero ¹²⁸, C. Ferrero ⁵⁵, A. Ferretti ²⁴, V.J.G. Feuillard ⁹⁴, V. Filova ³⁵, D. Finogeev ¹⁴⁰, F.M. Fionda ⁵¹, F. Flor ¹¹⁴, A.N. Flores ¹⁰⁸, S. Foertsch ⁶⁷, I. Fokin ⁹⁴, S. Fokin ¹⁴⁰, E. Fragiocomo ⁵⁶, E. Frajna ¹³⁶, U. Fuchs ³², N. Funicello ²⁸, C. Furget ⁷³, A. Furs ¹⁴⁰, T. Fusayasu ⁹⁸, J.J. Gaardhøje ⁸³, M. Gagliardi ²⁴, A.M. Gago ¹⁰¹, C.D. Galvan ¹⁰⁹, D.R. Gangadharan ¹¹⁴, P. Ganoti ⁷⁸, C. Garabatos ⁹⁷, J.R.A. Garcia ⁴⁴, E. Garcia-Solis ⁹, C. Gargiulo ³², A. Garibaldi ⁸¹, K. Garner ¹³⁵, P. Gasik ⁹⁷, A. Gautam ¹¹⁶, M.B. Gay Ducati ⁶⁵, M. Germain ¹⁰³, A. Ghimouz ¹²³, C. Ghosh ¹³², M. Giacalone ^{50,25}, P. Giubellino ^{97,55}, P. Giubilato ²⁷, A.M.C. Glaenzer ¹²⁸, P. Glässsel ⁹⁴, E. Glimos ¹²⁰, D.J.Q. Goh ⁷⁶, V. Gonzalez ¹³⁴, S. Gorbenov ³⁸, M. Gorgon ², K. Goswami ⁴⁷, S. Gotovac ³³, V. Grabski ⁶⁶, L.K. Graczykowski ¹³³, E. Grecka ⁸⁶, A. Grelli ⁵⁸, C. Grigoras ³², V. Grigoriev ¹⁴⁰, S. Grigoryan ^{141,1}, F. Grossa ³², J.F. Grosse-Oetringhaus ³², R. Grossi ⁹⁷, D. Grund ³⁵, G.G. Guardiano ¹¹¹, R. Guernane ⁷³, M. Guilbaud ¹⁰³, K. Gulbrandsen ⁸³, T. Gundem ⁶³, T. Gunji ¹²², W. Guo ⁶, A. Gupta ⁹¹, R. Gupta ⁹¹, R. Gupta ⁴⁷, S.P. Guzman ⁴⁴, K. Gwizdziel ¹³³, L. Gyulai ¹³⁶

- M.K. Habib⁹⁷, C. Hadjidakis $\textcolor{blue}{\bullet}$ ⁷², F.U. Haider $\textcolor{blue}{\bullet}$ ⁹¹, H. Hamagaki $\textcolor{blue}{\bullet}$ ⁷⁶, A. Hamdi $\textcolor{blue}{\bullet}$ ⁷⁴, M. Hamid⁶, Y. Han $\textcolor{blue}{\bullet}$ ¹³⁸, B.G. Hanley $\textcolor{blue}{\bullet}$ ¹³⁴, R. Hannigan $\textcolor{blue}{\bullet}$ ¹⁰⁸, J. Hansen $\textcolor{blue}{\bullet}$ ⁷⁵, M.R. Haque $\textcolor{blue}{\bullet}$ ¹³³, J.W. Harris $\textcolor{blue}{\bullet}$ ¹³⁷, A. Harton $\textcolor{blue}{\bullet}$ ⁹, H. Hassan $\textcolor{blue}{\bullet}$ ⁸⁷, D. Hatzifotiadou $\textcolor{blue}{\bullet}$ ⁵⁰, P. Hauer $\textcolor{blue}{\bullet}$ ⁴², L.B. Havener $\textcolor{blue}{\bullet}$ ¹³⁷, S.T. Heckel $\textcolor{blue}{\bullet}$ ⁹⁵, E. Hellbär $\textcolor{blue}{\bullet}$ ⁹⁷, H. Helstrup $\textcolor{blue}{\bullet}$ ³⁴, M. Hemmer $\textcolor{blue}{\bullet}$ ⁶³, T. Herman $\textcolor{blue}{\bullet}$ ³⁵, G. Herrera Corral $\textcolor{blue}{\bullet}$ ⁸, F. Herrmann¹³⁵, S. Herrmann $\textcolor{blue}{\bullet}$ ¹²⁶, K.F. Hetland $\textcolor{blue}{\bullet}$ ³⁴, B. Heybeck $\textcolor{blue}{\bullet}$ ⁶³, H. Hillemanns $\textcolor{blue}{\bullet}$ ³², B. Hippolyte $\textcolor{blue}{\bullet}$ ¹²⁷, F.W. Hoffmann $\textcolor{blue}{\bullet}$ ⁶⁹, B. Hofman $\textcolor{blue}{\bullet}$ ⁵⁸, B. Hohlweger $\textcolor{blue}{\bullet}$ ⁸⁴, G.H. Hong $\textcolor{blue}{\bullet}$ ¹³⁸, M. Horst $\textcolor{blue}{\bullet}$ ⁹⁵, A. Horzyk $\textcolor{blue}{\bullet}$ ², Y. Hou⁶, P. Hristov $\textcolor{blue}{\bullet}$ ³², C. Hughes $\textcolor{blue}{\bullet}$ ¹²⁰, P. Huhn⁶³, L.M. Huhta $\textcolor{blue}{\bullet}$ ¹¹⁵, T.J. Humanic $\textcolor{blue}{\bullet}$ ⁸⁸, L.A. Husova $\textcolor{blue}{\bullet}$ ¹³⁵, A. Hutson $\textcolor{blue}{\bullet}$ ¹¹⁴, R. Ilkaev¹⁴⁰, H. Ilyas $\textcolor{blue}{\bullet}$ ¹³, M. Inaba $\textcolor{blue}{\bullet}$ ¹²³, G.M. Innocenti $\textcolor{blue}{\bullet}$ ³², M. Ippolitov $\textcolor{blue}{\bullet}$ ¹⁴⁰, A. Isakov $\textcolor{blue}{\bullet}$ ⁸⁶, T. Isidori $\textcolor{blue}{\bullet}$ ¹¹⁶, M.S. Islam $\textcolor{blue}{\bullet}$ ⁹⁹, M. Ivanov¹², M. Ivanov⁹⁷, V. Ivanov $\textcolor{blue}{\bullet}$ ¹⁴⁰, K.E. Iversen $\textcolor{blue}{\bullet}$ ⁷⁵, M. Jablonski $\textcolor{blue}{\bullet}$ ², B. Jacak⁷⁴, N. Jacazio $\textcolor{blue}{\bullet}$ ²⁵, P.M. Jacobs $\textcolor{blue}{\bullet}$ ⁷⁴, S. Jadlovska¹⁰⁶, J. Jadlovsky¹⁰⁶, S. Jaelani $\textcolor{blue}{\bullet}$ ⁸², C. Jahnke¹¹¹, M.J. Jakubowska $\textcolor{blue}{\bullet}$ ¹³³, M.A. Janik $\textcolor{blue}{\bullet}$ ¹³³, T. Janson⁶⁹, M. Jercic⁸⁹, S. Ji $\textcolor{blue}{\bullet}$ ¹⁶, S. Jia¹⁰, A.A.P. Jimenez $\textcolor{blue}{\bullet}$ ⁶⁴, F. Jonas $\textcolor{blue}{\bullet}$ ⁸⁷, J.M. Jowett $\textcolor{blue}{\bullet}$ ^{32,97}, J. Jung $\textcolor{blue}{\bullet}$ ⁶³, M. Jung $\textcolor{blue}{\bullet}$ ⁶³, A. Junique $\textcolor{blue}{\bullet}$ ³², A. Jusko $\textcolor{blue}{\bullet}$ ¹⁰⁰, M.J. Kabus $\textcolor{blue}{\bullet}$ ^{32,133}, J. Kaewjai¹⁰⁵, P. Kalinak $\textcolor{blue}{\bullet}$ ⁵⁹, A.S. Kalteyer $\textcolor{blue}{\bullet}$ ⁹⁷, A. Kalweit $\textcolor{blue}{\bullet}$ ³², V. Kaplin $\textcolor{blue}{\bullet}$ ¹⁴⁰, A. Karasu Uysal $\textcolor{blue}{\bullet}$ ⁷¹, D. Karatovic $\textcolor{blue}{\bullet}$ ⁸⁹, O. Karavichev $\textcolor{blue}{\bullet}$ ¹⁴⁰, T. Karavicheva $\textcolor{blue}{\bullet}$ ¹⁴⁰, P. Karczmarczyk $\textcolor{blue}{\bullet}$ ¹³³, E. Karpechev $\textcolor{blue}{\bullet}$ ¹⁴⁰, U. Kebschull $\textcolor{blue}{\bullet}$ ⁶⁹, R. Keidel $\textcolor{blue}{\bullet}$ ¹³⁹, D.L.D. Keijdener⁵⁸, M. Keil $\textcolor{blue}{\bullet}$ ³², B. Ketzer $\textcolor{blue}{\bullet}$ ⁴², S.S. Khade $\textcolor{blue}{\bullet}$ ⁴⁷, A.M. Khan $\textcolor{blue}{\bullet}$ ⁶, S. Khan $\textcolor{blue}{\bullet}$ ¹⁵, A. Khanzadeev $\textcolor{blue}{\bullet}$ ¹⁴⁰, Y. Kharlov $\textcolor{blue}{\bullet}$ ¹⁴⁰, A. Khatun $\textcolor{blue}{\bullet}$ ¹¹⁶, A. Khuntia $\textcolor{blue}{\bullet}$ ¹⁰⁷, M.B. Kidson¹¹³, B. Kileng $\textcolor{blue}{\bullet}$ ³⁴, B. Kim $\textcolor{blue}{\bullet}$ ¹⁰⁴, C. Kim $\textcolor{blue}{\bullet}$ ¹⁶, D.J. Kim $\textcolor{blue}{\bullet}$ ¹¹⁵, E.J. Kim $\textcolor{blue}{\bullet}$ ⁶⁸, J. Kim $\textcolor{blue}{\bullet}$ ¹³⁸, J.S. Kim $\textcolor{blue}{\bullet}$ ⁴⁰, J. Kim $\textcolor{blue}{\bullet}$ ⁵⁷, J. Kim $\textcolor{blue}{\bullet}$ ⁶⁸, M. Kim $\textcolor{blue}{\bullet}$ ¹⁸, S. Kim $\textcolor{blue}{\bullet}$ ¹⁷, T. Kim $\textcolor{blue}{\bullet}$ ¹³⁸, K. Kimura $\textcolor{blue}{\bullet}$ ⁹², S. Kirsch $\textcolor{blue}{\bullet}$ ⁶³, I. Kisiel $\textcolor{blue}{\bullet}$ ³⁸, S. Kiselev $\textcolor{blue}{\bullet}$ ¹⁴⁰, A. Kisiel¹³³, J.P. Kitowski $\textcolor{blue}{\bullet}$ ², J.L. Klay $\textcolor{blue}{\bullet}$ ⁵, J. Klein $\textcolor{blue}{\bullet}$ ³², S. Klein $\textcolor{blue}{\bullet}$ ⁷⁴, C. Klein-Bösing $\textcolor{blue}{\bullet}$ ¹³⁵, M. Kleiner $\textcolor{blue}{\bullet}$ ⁶³, T. Klemenz $\textcolor{blue}{\bullet}$ ⁹⁵, A. Kluge $\textcolor{blue}{\bullet}$ ³², A.G. Knospe $\textcolor{blue}{\bullet}$ ¹¹⁴, C. Kobdaj $\textcolor{blue}{\bullet}$ ¹⁰⁵, T. Kollegger⁹⁷, A. Kondratyev $\textcolor{blue}{\bullet}$ ¹⁴¹, N. Kondratyeva $\textcolor{blue}{\bullet}$ ¹⁴⁰, E. Kondratyuk¹⁴⁰, J. Konig $\textcolor{blue}{\bullet}$ ⁶³, S.A. Konigstorfer $\textcolor{blue}{\bullet}$ ⁹⁵, P.J. Konopka $\textcolor{blue}{\bullet}$ ³², G. Kornakov $\textcolor{blue}{\bullet}$ ¹³³, S.D. Koryciak $\textcolor{blue}{\bullet}$ ², A. Kotliarov $\textcolor{blue}{\bullet}$ ⁸⁶, V. Kovalenko $\textcolor{blue}{\bullet}$ ¹⁴⁰, M. Kowalski $\textcolor{blue}{\bullet}$ ¹⁰⁷, V. Kozhuharov $\textcolor{blue}{\bullet}$ ³⁶, I. Králik $\textcolor{blue}{\bullet}$ ⁵⁹, A. Kravcákova $\textcolor{blue}{\bullet}$ ³⁷, L. Krcal $\textcolor{blue}{\bullet}$ ^{32,38}, M. Krivda $\textcolor{blue}{\bullet}$ ^{100,59}, F. Krizek $\textcolor{blue}{\bullet}$ ⁸⁶, K. Krizkova Gajdosova $\textcolor{blue}{\bullet}$ ³², M. Kroesen $\textcolor{blue}{\bullet}$ ⁹⁴, M. Krüger $\textcolor{blue}{\bullet}$ ⁶³, D.M. Krupova $\textcolor{blue}{\bullet}$ ³⁵, E. Kryshen $\textcolor{blue}{\bullet}$ ¹⁴⁰, V. Kučera $\textcolor{blue}{\bullet}$ ⁵⁷, C. Kuhn $\textcolor{blue}{\bullet}$ ¹²⁷, P.G. Kuijer $\textcolor{blue}{\bullet}$ ⁸⁴, T. Kumaoka¹²³, D. Kumar¹³², L. Kumar $\textcolor{blue}{\bullet}$ ⁹⁰, N. Kumar⁹⁰, S. Kumar $\textcolor{blue}{\bullet}$ ³¹, S. Kundu $\textcolor{blue}{\bullet}$ ³², P. Kurashvili $\textcolor{blue}{\bullet}$ ⁷⁹, A. Kurepin $\textcolor{blue}{\bullet}$ ¹⁴⁰, A.B. Kurepin $\textcolor{blue}{\bullet}$ ¹⁴⁰, A. Kuryakin¹⁴⁰, S. Kushpil $\textcolor{blue}{\bullet}$ ⁸⁶, J. Kvapil $\textcolor{blue}{\bullet}$ ¹⁰⁰, M.J. Kweon $\textcolor{blue}{\bullet}$ ⁵⁷, Y. Kwon $\textcolor{blue}{\bullet}$ ¹³⁸, S.L. La Pointe $\textcolor{blue}{\bullet}$ ³⁸, P. La Rocca $\textcolor{blue}{\bullet}$ ²⁶, A. Lakrathok¹⁰⁵, M. Lamanna $\textcolor{blue}{\bullet}$ ³², R. Langoy $\textcolor{blue}{\bullet}$ ¹¹⁹, P. Larionov $\textcolor{blue}{\bullet}$ ³², E. Laudi $\textcolor{blue}{\bullet}$ ³², L. Lautner $\textcolor{blue}{\bullet}$ ^{32,95}, R. Lavicka $\textcolor{blue}{\bullet}$ ¹⁰², R. Lea $\textcolor{blue}{\bullet}$ ^{131,54}, H. Lee $\textcolor{blue}{\bullet}$ ¹⁰⁴, I. Legrand $\textcolor{blue}{\bullet}$ ⁴⁵, G. Legras $\textcolor{blue}{\bullet}$ ¹³⁵, J. Lehrbach $\textcolor{blue}{\bullet}$ ³⁸, T.M. Lelek², R.C. Lemmon $\textcolor{blue}{\bullet}$ ⁸⁵, I. León Monzón $\textcolor{blue}{\bullet}$ ¹⁰⁹, M.M. Lesch $\textcolor{blue}{\bullet}$ ⁹⁵, E.D. Lesser $\textcolor{blue}{\bullet}$ ¹⁸, P. Lévai $\textcolor{blue}{\bullet}$ ¹³⁶, X. Li¹⁰, X.L. Li⁶, J. Lien $\textcolor{blue}{\bullet}$ ¹¹⁹, R. Lietava $\textcolor{blue}{\bullet}$ ¹⁰⁰, I. Likmeta $\textcolor{blue}{\bullet}$ ¹¹⁴, B. Lim $\textcolor{blue}{\bullet}$ ²⁴, S.H. Lim $\textcolor{blue}{\bullet}$ ¹⁶, V. Lindenstruth $\textcolor{blue}{\bullet}$ ³⁸, A. Lindner⁴⁵, C. Lippmann $\textcolor{blue}{\bullet}$ ⁹⁷, A. Liu $\textcolor{blue}{\bullet}$ ¹⁸, D.H. Liu $\textcolor{blue}{\bullet}$ ⁶, J. Liu $\textcolor{blue}{\bullet}$ ¹¹⁷, G.S.S. Liveraro¹¹¹, I.M. Lofnes $\textcolor{blue}{\bullet}$ ²⁰, C. Loizides $\textcolor{blue}{\bullet}$ ⁸⁷, S. Lokos $\textcolor{blue}{\bullet}$ ¹⁰⁷, J. Lomker $\textcolor{blue}{\bullet}$ ⁵⁸, P. Loncar $\textcolor{blue}{\bullet}$ ³³, J.A. Lopez $\textcolor{blue}{\bullet}$ ⁹⁴, X. Lopez $\textcolor{blue}{\bullet}$ ¹²⁵, E. López Torres $\textcolor{blue}{\bullet}$ ⁷, P. Lu $\textcolor{blue}{\bullet}$ ^{97,118}, J.R. Luhder $\textcolor{blue}{\bullet}$ ¹³⁵, M. Lunardon $\textcolor{blue}{\bullet}$ ²⁷, G. Luparello $\textcolor{blue}{\bullet}$ ⁵⁶, Y.G. Ma $\textcolor{blue}{\bullet}$ ³⁹, M. Mager $\textcolor{blue}{\bullet}$ ³², A. Maire $\textcolor{blue}{\bullet}$ ¹²⁷, M.V. Makariev $\textcolor{blue}{\bullet}$ ³⁶, M. Malaev $\textcolor{blue}{\bullet}$ ¹⁴⁰, G. Malfattore $\textcolor{blue}{\bullet}$ ²⁵, N.M. Malik $\textcolor{blue}{\bullet}$ ⁹¹, Q.W. Malik¹⁹, S.K. Malik $\textcolor{blue}{\bullet}$ ⁹¹, L. Malinina $\textcolor{blue}{\bullet}$ ^{VI,141}, D. Mallick $\textcolor{blue}{\bullet}$ ⁸⁰, N. Mallick $\textcolor{blue}{\bullet}$ ⁴⁷, G. Mandaglio $\textcolor{blue}{\bullet}$ ^{30,52}, S.K. Mandal $\textcolor{blue}{\bullet}$ ⁷⁹, V. Manko $\textcolor{blue}{\bullet}$ ¹⁴⁰, F. Manso $\textcolor{blue}{\bullet}$ ¹²⁵, V. Manzari $\textcolor{blue}{\bullet}$ ⁴⁹, Y. Mao $\textcolor{blue}{\bullet}$ ⁶, R.W. Marcjan $\textcolor{blue}{\bullet}$ ², G.V. Margagliotti $\textcolor{blue}{\bullet}$ ²³, A. Margotti $\textcolor{blue}{\bullet}$ ⁵⁰, A. Marín $\textcolor{blue}{\bullet}$ ⁹⁷, C. Markert $\textcolor{blue}{\bullet}$ ¹⁰⁸, P. Martinengo $\textcolor{blue}{\bullet}$ ³², M.I. Martínez $\textcolor{blue}{\bullet}$ ⁴⁴, G. Martínez García $\textcolor{blue}{\bullet}$ ¹⁰³, M.P.P. Martins $\textcolor{blue}{\bullet}$ ¹¹⁰, S. Masciocchi $\textcolor{blue}{\bullet}$ ⁹⁷, M. Masera $\textcolor{blue}{\bullet}$ ²⁴, A. Masoni $\textcolor{blue}{\bullet}$ ⁵¹, L. Massacrier $\textcolor{blue}{\bullet}$ ⁷², A. Mastroserio $\textcolor{blue}{\bullet}$ ^{129,49}, O. Matonoha $\textcolor{blue}{\bullet}$ ⁷⁵, S. Mattiazzo $\textcolor{blue}{\bullet}$ ²⁷, P.F.T. Matuoka¹¹⁰, A. Matyja $\textcolor{blue}{\bullet}$ ¹⁰⁷, C. Mayer $\textcolor{blue}{\bullet}$ ¹⁰⁷, A.L. Mazuecos $\textcolor{blue}{\bullet}$ ³², F. Mazzaschi $\textcolor{blue}{\bullet}$ ²⁴, M. Mazzilli $\textcolor{blue}{\bullet}$ ³², J.E. Mdhluli $\textcolor{blue}{\bullet}$ ¹²¹, A.F. Mechler⁶³, Y. Melikyan $\textcolor{blue}{\bullet}$ ^{43,140}, A. Menchaca-Rocha $\textcolor{blue}{\bullet}$ ⁶⁶, E. Meninno $\textcolor{blue}{\bullet}$ ^{102,28}, A.S. Menon¹¹⁴, M. Meres $\textcolor{blue}{\bullet}$ ¹², S. Mhlanga^{113,67}, Y. Miake¹²³, L. Micheletti $\textcolor{blue}{\bullet}$ ³², L.C. Migliorin¹²⁶, D.L. Mihaylov $\textcolor{blue}{\bullet}$ ⁹⁵, K. Mikhaylov $\textcolor{blue}{\bullet}$ ^{141,140}, A.N. Mishra $\textcolor{blue}{\bullet}$ ¹³⁶, D. Miśkowiec $\textcolor{blue}{\bullet}$ ⁹⁷, A. Modak $\textcolor{blue}{\bullet}$ ⁴, A.P. Mohanty $\textcolor{blue}{\bullet}$ ⁵⁸, B. Mohanty $\textcolor{blue}{\bullet}$ ⁸⁰, M. Mohisin Khan $\textcolor{blue}{\bullet}$ ^{III,15}, M.A. Molander $\textcolor{blue}{\bullet}$ ⁴³, Z. Moravcova $\textcolor{blue}{\bullet}$ ⁸³, C. Mordasini $\textcolor{blue}{\bullet}$ ⁹⁵, D.A. Moreira De Godoy¹³⁵, I. Morozov $\textcolor{blue}{\bullet}$ ¹⁴⁰, A. Morsch $\textcolor{blue}{\bullet}$ ³², T. Mrnjavac $\textcolor{blue}{\bullet}$ ³², V. Muccifora $\textcolor{blue}{\bullet}$ ⁴⁸, S. Muhuri $\textcolor{blue}{\bullet}$ ¹³², J.D. Mulligan $\textcolor{blue}{\bullet}$ ⁷⁴, A. Mulliri²², M.G. Munhoz $\textcolor{blue}{\bullet}$ ¹¹⁰, R.H. Munzer $\textcolor{blue}{\bullet}$ ⁶³, H. Murakami $\textcolor{blue}{\bullet}$ ¹²², S. Murray $\textcolor{blue}{\bullet}$ ¹¹³, L. Musa $\textcolor{blue}{\bullet}$ ³², J. Musinsky $\textcolor{blue}{\bullet}$ ⁵⁹, J.W. Myrcha¹³³, B. Naik $\textcolor{blue}{\bullet}$ ¹²¹, A.I. Nambrath $\textcolor{blue}{\bullet}$ ¹⁸, B.K. Nandi⁴⁶, R. Nania $\textcolor{blue}{\bullet}$ ⁵⁰, E. Nappi $\textcolor{blue}{\bullet}$ ⁴⁹, A.F. Nassirpour $\textcolor{blue}{\bullet}$ ^{17,75}, A. Nath $\textcolor{blue}{\bullet}$ ⁹⁴, C. Nattrass $\textcolor{blue}{\bullet}$ ¹²⁰, M.N. Naydenov $\textcolor{blue}{\bullet}$ ³⁶, A. Neagu¹⁹, A. Negru¹²⁴, L. Nellen $\textcolor{blue}{\bullet}$ ⁶⁴, G. Neskovic $\textcolor{blue}{\bullet}$ ³⁸, B.S. Nielsen $\textcolor{blue}{\bullet}$ ⁸³, E.G. Nielsen $\textcolor{blue}{\bullet}$ ⁸³, S. Nikolaev $\textcolor{blue}{\bullet}$ ¹⁴⁰, S. Nikulin $\textcolor{blue}{\bullet}$ ¹⁴⁰, V. Nikulin $\textcolor{blue}{\bullet}$ ¹⁴⁰, F. Noferini $\textcolor{blue}{\bullet}$ ⁵⁰, S. Noh $\textcolor{blue}{\bullet}$ ¹¹, P. Nomokonov $\textcolor{blue}{\bullet}$ ¹⁴¹, J. Norman $\textcolor{blue}{\bullet}$ ¹¹⁷, N. Novitzky $\textcolor{blue}{\bullet}$ ¹²³, P. Nowakowski $\textcolor{blue}{\bullet}$ ¹³³, A. Nyanin $\textcolor{blue}{\bullet}$ ¹⁴⁰, J. Nystrand $\textcolor{blue}{\bullet}$ ²⁰, M. Ogino⁷⁶, A. Ohlson $\textcolor{blue}{\bullet}$ ⁷⁵, V.A. Okorokov $\textcolor{blue}{\bullet}$ ¹⁴⁰, J. Oleniacz $\textcolor{blue}{\bullet}$ ¹³³, A.C. Oliveira Da Silva $\textcolor{blue}{\bullet}$ ¹²⁰, M.H. Oliver $\textcolor{blue}{\bullet}$ ¹³⁷, A. Onnerstad $\textcolor{blue}{\bullet}$ ¹¹⁵, C. Oppedisano $\textcolor{blue}{\bullet}$ ⁵⁵, A. Ortiz Velasquez $\textcolor{blue}{\bullet}$ ⁶⁴, J. Otwinowski $\textcolor{blue}{\bullet}$ ¹⁰⁷, M. Oya⁹², K. Oyama $\textcolor{blue}{\bullet}$ ⁷⁶, Y. Pachmayer $\textcolor{blue}{\bullet}$ ⁹⁴, S. Padhan⁴⁶, D. Pagano $\textcolor{blue}{\bullet}$ ^{131,54}, G. Paić $\textcolor{blue}{\bullet}$ ⁶⁴, A. Palasciano $\textcolor{blue}{\bullet}$ ⁴⁹, S. Panebianco $\textcolor{blue}{\bullet}$ ¹²⁸, H. Park $\textcolor{blue}{\bullet}$ ¹²³, H. Park $\textcolor{blue}{\bullet}$ ¹⁰⁴, J. Park $\textcolor{blue}{\bullet}$ ⁵⁷, J.E. Parkkila $\textcolor{blue}{\bullet}$ ³², R.N. Patra⁹¹, B. Paul $\textcolor{blue}{\bullet}$ ²², H. Pei $\textcolor{blue}{\bullet}$ ⁶, T. Peitzmann $\textcolor{blue}{\bullet}$ ⁵⁸, X. Peng $\textcolor{blue}{\bullet}$ ⁶, M. Pennisi $\textcolor{blue}{\bullet}$ ²⁴,

- D. Peresunko ¹⁴⁰, G.M. Perez ⁷, S. Perrin ¹²⁸, Y. Pestov ¹⁴⁰, V. Petrov ¹⁴⁰, M. Petrovici ⁴⁵, R.P. Pezzi ^{103,65}, S. Piano ⁵⁶, M. Pikna ¹², P. Pillot ¹⁰³, O. Pinazza ^{50,32}, L. Pinsky ¹¹⁴, C. Pinto ⁹⁵, S. Pisano ⁴⁸, M. Płoskoń ⁷⁴, M. Planinic ⁸⁹, F. Pliquet ⁶³, M.G. Poghosyan ⁸⁷, B. Polichtchouk ¹⁴⁰, S. Politano ²⁹, N. Poljak ⁸⁹, A. Pop ⁴⁵, S. Portebœuf-Houssais ¹²⁵, V. Pozdniakov ¹⁴¹, I.Y. Pozos ⁴⁴, K.K. Pradhan ⁴⁷, S.K. Prasad ⁴, S. Prasad ⁴⁷, R. Pregenella ⁵⁰, F. Prino ⁵⁵, C.A. Pruneau ¹³⁴, I. Pshenichnov ¹⁴⁰, M. Puccio ³², S. Pucillo ²⁴, Z. Pugelova ¹⁰⁶, S. Qiu ⁸⁴, L. Quaglia ²⁴, R.E. Quishpe ¹¹⁴, S. Ragoni ¹⁴, A. Rakotozafindrabe ¹²⁸, L. Ramello ^{130,55}, F. Rami ¹²⁷, S.A.R. Ramirez ⁴⁴, T.A. Rancien ⁷³, M. Rasa ²⁶, S.S. Räsänen ⁴³, R. Rath ⁵⁰, M.P. Rauch ²⁰, I. Ravasenga ⁸⁴, K.F. Read ^{87,120}, C. Reckziegel ¹¹², A.R. Redelbach ³⁸, K. Redlich ^{IV,79}, C.A. Reetz ⁹⁷, A. Rehman ²⁰, F. Reidt ³², H.A. Reme-Ness ³⁴, Z. Rescakova ³⁷, K. Reygers ⁹⁴, A. Riabov ¹⁴⁰, V. Riabov ¹⁴⁰, R. Ricci ²⁸, M. Richter ¹⁹, A.A. Riedel ⁹⁵, W. Riegler ³², C. Ristea ⁶², M.V. Rodriguez ³², M. Rodríguez Cahuantzi ⁴⁴, K. Røed ¹⁹, R. Rogalev ¹⁴⁰, E. Rogochaya ¹⁴¹, T.S. Rogoschinski ⁶³, D. Rohr ³², D. Röhrlach ²⁰, P.F. Rojas ⁴⁴, S. Rojas Torres ³⁵, P.S. Rokita ¹³³, G. Romanenko ¹⁴¹, F. Ronchetti ⁴⁸, A. Rosano ^{30,52}, E.D. Rosas ⁶⁴, K. Roslon ¹³³, A. Rossi ⁵³, A. Roy ⁴⁷, S. Roy ⁴⁶, N. Rubin ²⁵, O.V. Rueda ¹¹⁴, D. Ruggiano ¹³³, R. Rui ²³, P.G. Russek ², R. Russo ⁸⁴, A. Rustamov ⁸¹, E. Ryabinkin ¹⁴⁰, Y. Ryabov ¹⁴⁰, A. Rybicki ¹⁰⁷, H. Rytkonen ¹¹⁵, J. Ryu ¹⁶, W. Rzesz ¹³³, O.A.M. Saarimaki ⁴³, R. Sadek ¹⁰³, S. Sadhu ³¹, S. Sadovsky ¹⁴⁰, J. Saetre ²⁰, K. Šafařík ³⁵, P. Saha ⁴¹, S.K. Saha ⁴, S. Saha ⁸⁰, B. Sahoo ⁴⁶, B. Sahoo ⁴⁷, R. Sahoo ⁴⁷, S. Sahoo ⁶⁰, D. Sahu ⁴⁷, P.K. Sahu ⁶⁰, J. Saini ¹³², K. Sajdakova ³⁷, S. Sakai ¹²³, M.P. Salvan ⁹⁷, S. Sambyal ⁹¹, I. Sanna ^{32,95}, T.B. Saramela ¹¹⁰, D. Sarkar ¹³⁴, N. Sarkar ¹³², P. Sarma ⁴¹, V. Sarritzu ²², V.M. Sarti ⁹⁵, M.H.P. Sas ¹³⁷, J. Schambach ⁸⁷, H.S. Scheid ⁶³, C. Schiaua ⁴⁵, R. Schicker ⁹⁴, A. Schmah ⁹⁴, C. Schmidt ⁹⁷, H.R. Schmidt ⁹³, M.O. Schmidt ³², M. Schmidt ⁹³, N.V. Schmidt ⁸⁷, A.R. Schmier ¹²⁰, R. Schotter ¹²⁷, A. Schröter ³⁸, J. Schukraft ³², K. Schwarz ⁹⁷, K. Schweda ⁹⁷, G. Scioli ²⁵, E. Scomparin ⁵⁵, J.E. Seger ¹⁴, Y. Sekiguchi ¹²², D. Sekihata ¹²², I. Selyuzhenkov ⁹⁷, S. Senyukov ¹²⁷, J.J. Seo ⁵⁷, D. Serebryakov ¹⁴⁰, L. Šerkšnytė ⁹⁵, A. Sevcenco ⁶², T.J. Shaba ⁶⁷, A. Shabetai ¹⁰³, R. Shahoyan ³², A. Shangaraev ¹⁴⁰, A. Sharma ⁹⁰, B. Sharma ⁹¹, D. Sharma ⁴⁶, H. Sharma ^{53,107}, M. Sharma ⁹¹, S. Sharma ⁷⁶, S. Sharma ⁹¹, U. Sharma ⁹¹, A. Shatat ⁷², O. Sheibani ¹¹⁴, K. Shigaki ⁹², M. Shimomura ⁷⁷, J. Shin ¹¹, S. Shirinkin ¹⁴⁰, Q. Shou ³⁹, Y. Sibirjak ¹⁴⁰, S. Siddhanta ⁵¹, T. Siemarczuk ⁷⁹, T.F. Silva ¹¹⁰, D. Silvermyr ⁷⁵, T. Simantathammakul ¹⁰⁵, R. Simeonov ³⁶, B. Singh ⁹¹, B. Singh ⁹⁵, K. Singh ⁴⁷, R. Singh ⁸⁰, R. Singh ⁹¹, R. Singh ⁴⁷, S. Singh ¹⁵, V.K. Singh ¹³², V. Singhal ¹³², T. Sinha ⁹⁹, B. Sitar ¹², M. Sitta ^{130,55}, T.B. Skaali ¹⁹, G. Skorodumovs ⁹⁴, M. Slupecki ⁴³, N. Smirnov ¹³⁷, R.J.M. Snellings ⁵⁸, E.H. Solheim ¹⁹, J. Song ¹¹⁴, A. Songmoolnak ¹⁰⁵, C. Sonnabend ^{32,97}, F. Soramel ²⁷, A.B. Soto-hernandez ⁸⁸, R. Spijkers ⁸⁴, I. Sputowska ¹⁰⁷, J. Staa ⁷⁵, J. Stachel ⁹⁴, I. Stan ⁶², P.J. Steffanic ¹²⁰, S.F. Stiefelmaier ⁹⁴, D. Stocco ¹⁰³, I. Storehaug ¹⁹, P. Stratmann ¹³⁵, S. Strazzi ²⁵, C.P. Stylianidis ⁸⁴, A.A.P. Suwaide ¹¹⁰, C. Suire ⁷², M. Sukhanov ¹⁴⁰, M. Suljic ³², R. Sultanov ¹⁴⁰, V. Sumberia ⁹¹, S. Sumowidagdo ⁸², S. Swain ⁶⁰, I. Szarka ¹², M. Szymkowski ¹³³, S.F. Taghavi ⁹⁵, G. Taillepied ⁹⁷, J. Takahashi ¹¹¹, G.J. Tambave ⁸⁰, S. Tang ⁶, Z. Tang ¹¹⁸, J.D. Tapia Takaki ^{V,116}, N. Tapus ¹²⁴, M.G. Tarzila ⁴⁵, G.F. Tassielli ³¹, A. Tauro ³², G. Tejeda Muñoz ⁴⁴, A. Telesca ³², L. Terlizzi ²⁴, C. Terrevoli ¹¹⁴, S. Thakur ⁴, D. Thomas ¹⁰⁸, A. Tikhonov ¹⁴⁰, A.R. Timmins ¹¹⁴, M. Tkacik ¹⁰⁶, T. Tkacik ¹⁰⁶, A. Toia ⁶³, R. Tokumoto ⁹², N. Topilskaya ¹⁴⁰, M. Toppi ⁴⁸, T. Tork ⁷², A.G. Torres Ramos ³¹, A. Trifiró ^{30,52}, A.S. Triolo ^{32,30,52}, S. Tripathy ⁵⁰, T. Tripathy ⁴⁶, S. Trogolo ³², V. Trubnikov ³, W.H. Trzaska ¹¹⁵, T.P. Trzciński ¹³³, A. Tumkin ¹⁴⁰, R. Turrisi ⁵³, T.S. Tveter ¹⁹, K. Ullaland ²⁰, B. Ulukutlu ⁹⁵, A. Uras ¹²⁶, M. Urioni ^{54,131}, G.L. Usai ²², M. Vala ³⁷, N. Valle ²¹, L.V.R. van Doremalen ⁵⁸, M. van Leeuwen ⁸⁴, C.A. van Veen ⁹⁴, R.J.G. van Weelden ⁸⁴, P. Vande Vyvre ³², D. Varga ¹³⁶, Z. Varga ¹³⁶, M. Vasileiou ⁷⁸, A. Vasiliev ¹⁴⁰, O. Vázquez Doce ⁴⁸, V. Vechernin ¹⁴⁰, E. Vercellin ²⁴, S. Vergara Limón ⁴⁴, L. Vermunt ⁹⁷, R. Vértesi ¹³⁶, M. Verweij ⁵⁸, L. Vickovic ³³, Z. Vilakazi ¹²¹, O. Villalobos Baillie ¹⁰⁰, A. Villani ²³, G. Vino ⁴⁹, A. Vinogradov ¹⁴⁰, T. Virgili ²⁸, M.M.O. Virta ¹¹⁵, V. Vislavicius ⁷⁵, A. Vodopyanov ¹⁴¹, B. Volkel ³², M.A. Völk ⁹⁴, K. Voloshin ¹⁴⁰, S.A. Voloshin ¹³⁴, G. Volpe ³¹, B. von Haller ³², I. Vorobyev ⁹⁵, N. Vozniuk ¹⁴⁰, J. Vrláková ³⁷, J. Wan ³⁹, C. Wang ³⁹, D. Wang ³⁹, Y. Wang ³⁹, A. Wegrzynek ³², F.T. Weiglhofer ³⁸, S.C. Wenzel ³², J.P. Wessels ¹³⁵, S.L. Weyhmiller ¹³⁷, J. Wiechula ⁶³, J. Wikne ¹⁹, G. Wilk ⁷⁹, J. Wilkinson ⁹⁷, G.A. Willems ¹³⁵, B. Windelband ⁹⁴, M. Winn ¹²⁸, J.R. Wright ¹⁰⁸, W. Wu ³⁹, Y. Wu ¹¹⁸, R. Xu ⁶, A. Yadav ⁴², A.K. Yadav ¹³², S. Yalcin ⁷¹, Y. Yamaguchi ⁹², S. Yang ²⁰, S. Yano ⁹², Z. Yin ⁶, I.-K. Yoo ¹⁶, J.H. Yoon ⁵⁷, H. Yu ¹¹, S. Yuan ²⁰, A. Yuncu ⁹⁴, V. Zaccolo ²³, C. Zampolli ³², F. Zanone ⁹⁴, N. Zardoshti ³², A. Zarochentsev ¹⁴⁰, P. Závada ⁶¹, N. Zaviyalov ¹⁴⁰, M. Zhalov ¹⁴⁰, B. Zhang ⁶, L. Zhang ³⁹, S. Zhang ³⁹, X. Zhang ⁶,

Y. Zhang¹¹⁸, Z. Zhang⁶, M. Zhao¹⁰, V. Zhrebchevskii¹⁴⁰, Y. Zhi¹⁰, D. Zhou⁶, Y. Zhou⁸³,
 J. Zhu^{97,6}, Y. Zhu⁶, S.C. Zugravel⁵⁵, N. Zurlo^{131,54}

Affiliation Notes

^I Deceased

^{II} Also at: Italian National Agency for New Technologies, Energy and Sustainable Economic Development (ENEA), Bologna, Italy

^{III} Also at: Department of Applied Physics, Aligarh Muslim University, Aligarh, India

^{IV} Also at: Institute of Theoretical Physics, University of Wroclaw, Poland

^V Also at: University of Kansas, Lawrence, Kansas, United States

^{VI} Also at: An institution covered by a cooperation agreement with CERN

Collaboration Institutes

¹ A.I. Alikhanyan National Science Laboratory (Yerevan Physics Institute) Foundation, Yerevan, Armenia

² AGH University of Science and Technology, Cracow, Poland

³ Bogolyubov Institute for Theoretical Physics, National Academy of Sciences of Ukraine, Kiev, Ukraine

⁴ Bose Institute, Department of Physics and Centre for Astroparticle Physics and Space Science (CAPSS), Kolkata, India

⁵ California Polytechnic State University, San Luis Obispo, California, United States

⁶ Central China Normal University, Wuhan, China

⁷ Centro de Aplicaciones Tecnológicas y Desarrollo Nuclear (CEADEN), Havana, Cuba

⁸ Centro de Investigación y de Estudios Avanzados (CINVESTAV), Mexico City and Mérida, Mexico

⁹ Chicago State University, Chicago, Illinois, United States

¹⁰ China Institute of Atomic Energy, Beijing, China

¹¹ Chungbuk National University, Cheongju, Republic of Korea

¹² Comenius University Bratislava, Faculty of Mathematics, Physics and Informatics, Bratislava, Slovak Republic

¹³ COMSATS University Islamabad, Islamabad, Pakistan

¹⁴ Creighton University, Omaha, Nebraska, United States

¹⁵ Department of Physics, Aligarh Muslim University, Aligarh, India

¹⁶ Department of Physics, Pusan National University, Pusan, Republic of Korea

¹⁷ Department of Physics, Sejong University, Seoul, Republic of Korea

¹⁸ Department of Physics, University of California, Berkeley, California, United States

¹⁹ Department of Physics, University of Oslo, Oslo, Norway

²⁰ Department of Physics and Technology, University of Bergen, Bergen, Norway

²¹ Dipartimento di Fisica, Università di Pavia, Pavia, Italy

²² Dipartimento di Fisica dell’Università and Sezione INFN, Cagliari, Italy

²³ Dipartimento di Fisica dell’Università and Sezione INFN, Trieste, Italy

²⁴ Dipartimento di Fisica dell’Università and Sezione INFN, Turin, Italy

²⁵ Dipartimento di Fisica e Astronomia dell’Università and Sezione INFN, Bologna, Italy

²⁶ Dipartimento di Fisica e Astronomia dell’Università and Sezione INFN, Catania, Italy

²⁷ Dipartimento di Fisica e Astronomia dell’Università and Sezione INFN, Padova, Italy

²⁸ Dipartimento di Fisica ‘E.R. Caianiello’ dell’Università and Gruppo Collegato INFN, Salerno, Italy

²⁹ Dipartimento DISAT del Politecnico and Sezione INFN, Turin, Italy

³⁰ Dipartimento di Scienze MIFT, Università di Messina, Messina, Italy

³¹ Dipartimento Interateneo di Fisica ‘M. Merlin’ and Sezione INFN, Bari, Italy

³² European Organization for Nuclear Research (CERN), Geneva, Switzerland

³³ Faculty of Electrical Engineering, Mechanical Engineering and Naval Architecture, University of Split, Split, Croatia

³⁴ Faculty of Engineering and Science, Western Norway University of Applied Sciences, Bergen, Norway

³⁵ Faculty of Nuclear Sciences and Physical Engineering, Czech Technical University in Prague, Prague, Czech Republic

³⁶ Faculty of Physics, Sofia University, Sofia, Bulgaria

³⁷ Faculty of Science, P.J. Šafárik University, Košice, Slovak Republic

³⁸ Frankfurt Institute for Advanced Studies, Johann Wolfgang Goethe-Universität Frankfurt, Frankfurt, Germany

- ³⁹ Fudan University, Shanghai, China
⁴⁰ Gangneung-Wonju National University, Gangneung, Republic of Korea
⁴¹ Gauhati University, Department of Physics, Guwahati, India
⁴² Helmholtz-Institut für Strahlen- und Kernphysik, Rheinische Friedrich-Wilhelms-Universität Bonn, Bonn, Germany
⁴³ Helsinki Institute of Physics (HIP), Helsinki, Finland
⁴⁴ High Energy Physics Group, Universidad Autónoma de Puebla, Puebla, Mexico
⁴⁵ Horia Hulubei National Institute of Physics and Nuclear Engineering, Bucharest, Romania
⁴⁶ Indian Institute of Technology Bombay (IIT), Mumbai, India
⁴⁷ Indian Institute of Technology Indore, Indore, India
⁴⁸ INFN, Laboratori Nazionali di Frascati, Frascati, Italy
⁴⁹ INFN, Sezione di Bari, Bari, Italy
⁵⁰ INFN, Sezione di Bologna, Bologna, Italy
⁵¹ INFN, Sezione di Cagliari, Cagliari, Italy
⁵² INFN, Sezione di Catania, Catania, Italy
⁵³ INFN, Sezione di Padova, Padova, Italy
⁵⁴ INFN, Sezione di Pavia, Pavia, Italy
⁵⁵ INFN, Sezione di Torino, Turin, Italy
⁵⁶ INFN, Sezione di Trieste, Trieste, Italy
⁵⁷ Inha University, Incheon, Republic of Korea
⁵⁸ Institute for Gravitational and Subatomic Physics (GRASP), Utrecht University/Nikhef, Utrecht, Netherlands
⁵⁹ Institute of Experimental Physics, Slovak Academy of Sciences, Košice, Slovak Republic
⁶⁰ Institute of Physics, Homi Bhabha National Institute, Bhubaneswar, India
⁶¹ Institute of Physics of the Czech Academy of Sciences, Prague, Czech Republic
⁶² Institute of Space Science (ISS), Bucharest, Romania
⁶³ Institut für Kernphysik, Johann Wolfgang Goethe-Universität Frankfurt, Frankfurt, Germany
⁶⁴ Instituto de Ciencias Nucleares, Universidad Nacional Autónoma de México, Mexico City, Mexico
⁶⁵ Instituto de Física, Universidade Federal do Rio Grande do Sul (UFRGS), Porto Alegre, Brazil
⁶⁶ Instituto de Física, Universidad Nacional Autónoma de México, Mexico City, Mexico
⁶⁷ iThemba LABS, National Research Foundation, Somerset West, South Africa
⁶⁸ Jeonbuk National University, Jeonju, Republic of Korea
⁶⁹ Johann-Wolfgang-Goethe Universität Frankfurt Institut für Informatik, Fachbereich Informatik und Mathematik, Frankfurt, Germany
⁷⁰ Korea Institute of Science and Technology Information, Daejeon, Republic of Korea
⁷¹ KTO Karatay University, Konya, Turkey
⁷² Laboratoire de Physique des 2 Infinis, Irène Joliot-Curie, Orsay, France
⁷³ Laboratoire de Physique Subatomique et de Cosmologie, Université Grenoble-Alpes, CNRS-IN2P3, Grenoble, France
⁷⁴ Lawrence Berkeley National Laboratory, Berkeley, California, United States
⁷⁵ Lund University Department of Physics, Division of Particle Physics, Lund, Sweden
⁷⁶ Nagasaki Institute of Applied Science, Nagasaki, Japan
⁷⁷ Nara Women's University (NWU), Nara, Japan
⁷⁸ National and Kapodistrian University of Athens, School of Science, Department of Physics , Athens, Greece
⁷⁹ National Centre for Nuclear Research, Warsaw, Poland
⁸⁰ National Institute of Science Education and Research, Homi Bhabha National Institute, Jatni, India
⁸¹ National Nuclear Research Center, Baku, Azerbaijan
⁸² National Research and Innovation Agency - BRIN, Jakarta, Indonesia
⁸³ Niels Bohr Institute, University of Copenhagen, Copenhagen, Denmark
⁸⁴ Nikhef, National institute for subatomic physics, Amsterdam, Netherlands
⁸⁵ Nuclear Physics Group, STFC Daresbury Laboratory, Daresbury, United Kingdom
⁸⁶ Nuclear Physics Institute of the Czech Academy of Sciences, Husinec-Řež, Czech Republic
⁸⁷ Oak Ridge National Laboratory, Oak Ridge, Tennessee, United States
⁸⁸ Ohio State University, Columbus, Ohio, United States
⁸⁹ Physics department, Faculty of science, University of Zagreb, Zagreb, Croatia
⁹⁰ Physics Department, Panjab University, Chandigarh, India
⁹¹ Physics Department, University of Jammu, Jammu, India

- ⁹² Physics Program and International Institute for Sustainability with Knotted Chiral Meta Matter (SKCM2), Hiroshima University, Hiroshima, Japan
⁹³ Physikalisches Institut, Eberhard-Karls-Universität Tübingen, Tübingen, Germany
⁹⁴ Physikalisches Institut, Ruprecht-Karls-Universität Heidelberg, Heidelberg, Germany
⁹⁵ Physik Department, Technische Universität München, Munich, Germany
⁹⁶ Politecnico di Bari and Sezione INFN, Bari, Italy
⁹⁷ Research Division and ExtreMe Matter Institute EMMI, GSI Helmholtzzentrum für Schwerionenforschung GmbH, Darmstadt, Germany
⁹⁸ Saga University, Saga, Japan
⁹⁹ Saha Institute of Nuclear Physics, Homi Bhabha National Institute, Kolkata, India
¹⁰⁰ School of Physics and Astronomy, University of Birmingham, Birmingham, United Kingdom
¹⁰¹ Sección Física, Departamento de Ciencias, Pontificia Universidad Católica del Perú, Lima, Peru
¹⁰² Stefan Meyer Institut für Subatomare Physik (SMI), Vienna, Austria
¹⁰³ SUBATECH, IMT Atlantique, Nantes Université, CNRS-IN2P3, Nantes, France
¹⁰⁴ Sungkyunkwan University, Suwon City, Republic of Korea
¹⁰⁵ Suranaree University of Technology, Nakhon Ratchasima, Thailand
¹⁰⁶ Technical University of Košice, Košice, Slovak Republic
¹⁰⁷ The Henryk Niewodniczanski Institute of Nuclear Physics, Polish Academy of Sciences, Cracow, Poland
¹⁰⁸ The University of Texas at Austin, Austin, Texas, United States
¹⁰⁹ Universidad Autónoma de Sinaloa, Culiacán, Mexico
¹¹⁰ Universidade de São Paulo (USP), São Paulo, Brazil
¹¹¹ Universidade Estadual de Campinas (UNICAMP), Campinas, Brazil
¹¹² Universidade Federal do ABC, Santo Andre, Brazil
¹¹³ University of Cape Town, Cape Town, South Africa
¹¹⁴ University of Houston, Houston, Texas, United States
¹¹⁵ University of Jyväskylä, Jyväskylä, Finland
¹¹⁶ University of Kansas, Lawrence, Kansas, United States
¹¹⁷ University of Liverpool, Liverpool, United Kingdom
¹¹⁸ University of Science and Technology of China, Hefei, China
¹¹⁹ University of South-Eastern Norway, Kongsberg, Norway
¹²⁰ University of Tennessee, Knoxville, Tennessee, United States
¹²¹ University of the Witwatersrand, Johannesburg, South Africa
¹²² University of Tokyo, Tokyo, Japan
¹²³ University of Tsukuba, Tsukuba, Japan
¹²⁴ University Politehnica of Bucharest, Bucharest, Romania
¹²⁵ Université Clermont Auvergne, CNRS/IN2P3, LPC, Clermont-Ferrand, France
¹²⁶ Université de Lyon, CNRS/IN2P3, Institut de Physique des 2 Infinis de Lyon, Lyon, France
¹²⁷ Université de Strasbourg, CNRS, IPHC UMR 7178, F-67000 Strasbourg, France, Strasbourg, France
¹²⁸ Université Paris-Saclay Centre d'Etudes de Saclay (CEA), IRFU, Département de Physique Nucléaire (DPhN), Saclay, France
¹²⁹ Università degli Studi di Foggia, Foggia, Italy
¹³⁰ Università del Piemonte Orientale, Vercelli, Italy
¹³¹ Università di Brescia, Brescia, Italy
¹³² Variable Energy Cyclotron Centre, Homi Bhabha National Institute, Kolkata, India
¹³³ Warsaw University of Technology, Warsaw, Poland
¹³⁴ Wayne State University, Detroit, Michigan, United States
¹³⁵ Westfälische Wilhelms-Universität Münster, Institut für Kernphysik, Münster, Germany
¹³⁶ Wigner Research Centre for Physics, Budapest, Hungary
¹³⁷ Yale University, New Haven, Connecticut, United States
¹³⁸ Yonsei University, Seoul, Republic of Korea
¹³⁹ Zentrum für Technologie und Transfer (ZTT), Worms, Germany
¹⁴⁰ Affiliated with an institute covered by a cooperation agreement with CERN
¹⁴¹ Affiliated with an international laboratory covered by a cooperation agreement with CERN.